Hot July weekend made warmer and more likely due to climate change

Authors
Claire Bergin*, ICARUS Climate Research Centre, Maynooth University, Maynooth, Ireland*
Ben Clarke, *Centre for Environmental Policy, Imperial College, London, UK*
Pádraig Flattery*, Met Éireann, Glasnevin, Dublin 9, Ireland*
Ciarán Kelly*, Met Éireann, Glasnevin, Dublin 9, Ireland*
Peter Thorne*, ICARUS Climate Research Centre, Maynooth University, Maynooth, Ireland*

Review Authors
Clair Barnes, *Centre for Environmental Policy, Imperial College, London, UK*

Main findings

- The maximum temperatures on Friday 11 and Saturday 12 July would have been expected to occur on average once in every 14 years in the pre-industrial climate. Today, with 1.3°C of human-caused global warming, similar events are expected to occur once every 6 years.
- If warming reaches 2.6°C, which is expected this century under current policies, similar two-day periods of heat are expected to become a 1-in-3-year event.
- On July 12, temperatures across much of the country exceeded 28°C, and went as high as 31°C. These temperatures were made approximately 1.4°C warmer as a result of human-caused global warming. A similar increase in temperature was found for the two-day event.
- Specifically, looking at the high temperatures on Saturday the 12, they would have been expected to happen once in every 21 years in a 1.3°C cooler climate. Now, with human-caused global warming they are expected to happen once in every 8 years.
- A wide range of impacts highlight how extreme heat could be an emerging risk in Ireland. High night-time temperatures have potential dangerous effects for people with underlying health conditions if their bodies don't manage to properly rest and recover. Red level forest fire warnings underlined the increased fire threat experienced under rising temperatures. High temperatures also caused a section of road to melt in Co. Cork and also put a strain on an already struggling water supply network.

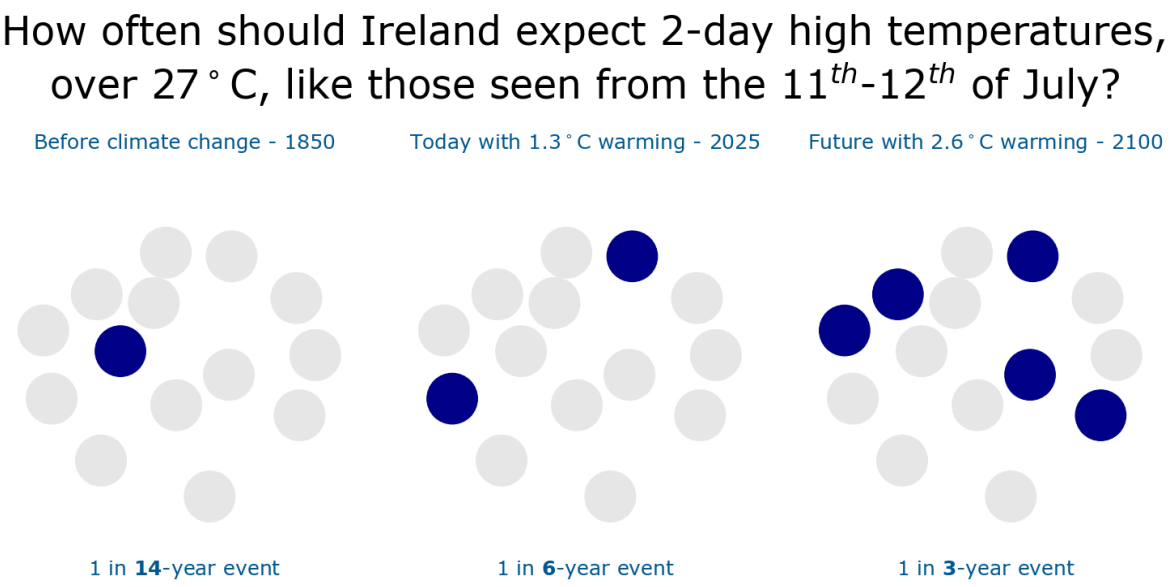

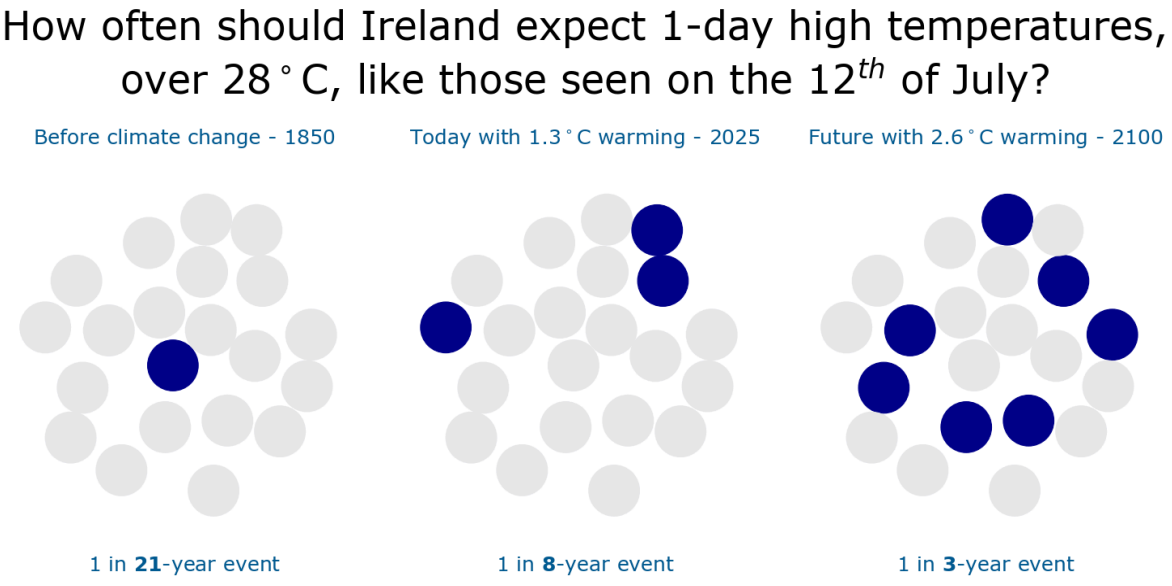

1 Introduction

On the 11th and 12th of July 2025, Ireland experienced unusually intense heat with temperatures reaching in excess of 27°C and breaking 30°C in parts of the country. Temperatures were highest on July 12th with a number of high-temperature warnings issued for the two days.

In the recent Ireland's Climate Change Assessment published in 2023 it was concluded that

'In Ireland annual average temperatures are now approximately 1.0°C higher than they were in the early 20th century. Sixteen of the top twenty warmest years since 1900 have occurred since 1990, with 2022 being the warmest year to date[1]. Centennial timescale changes in

[1] Note that 2023 then subsequently exceeded the 2022 value by a considerable margin.

Ireland are broadly consistent with global changes owing to our geographical situation between Europe (which is warming considerably faster than the global mean) and the North Atlantic (which is warming at a slower rate).'

The assessment further found that

'*Extremes of heat in Ireland (heatwaves) are becoming more frequent and more severe in line with global trends, while extremes of cold (cold waves) are becoming less frequent and less severe.*'

It also found that rare extreme heat events were projected to become more common. The range of climate models was shown to perform well in simulating temperatures across the island.

In the days leading up to the event, Met Éireann warned that temperatures may exceed 27°C across the country and possibly reach the low 30s on Saturday July 12th. This turned out to be the case for much of Ireland, with four weather stations registering above 30°C on Saturday. This summer has already seen higher than normal temperatures, with 29.6°C previously registered in Roscommon on the 30th of June. In contrast, the highest summertime temperature of the previous year, 2024, was 26.6°C. For context, the mean air temperature for summer (June, July and August) is 14.6°C, the average maximum temperatures are 18.6°C and average minimum temperatures are 10.7°C. For July in particular, the average maximum air temperature is 19.1°C. The current national maximum temperature record was in June 1887 and sits at 33.3°C (Kelly et al., 2025), with the second highest temperature of 33.0°C recorded in 2022. Thus, the 30°C temperatures recorded on the 12th of July are uncommon for Ireland.

Met Éireann also forecasted for nighttime temperatures to remain in the mid-teens for much of the country. A number of stations registered temperatures in excess of 15°C for the night of the 11th to 12th of July which is unusual for Ireland.

On the 11th of July, Phoenix Park, Co. Dublin, recorded a provisional maximum temperature of 29.0°C (8.8°C above its 1991–2020 long-term average (LTA)). The highest temperature of the period was observed on the 12th of July at Mount Dillon, Co. Roscommon, where 31.1°C was recorded (11.5°C above its LTA of 19.6°C). Elevated temperatures continued into the 13th of July, with Gurteen, Co. Tipperary, reaching 28.6°C (9.2°C above its LTA). Several Met Éireann stations provisionally recorded their highest July 00–00 maximum temperatures on record, including Malin Head (27.6°C) and Finner (29.6°C) in Co. Donegal, and Knock Airport, Co. Mayo (28.7°C). Monthly mean temperatures were among the warmest in recent decades at several long-term stations. For example, Dublin Airport, Co. Dublin recorded its warmest July in 12 years, while Malin Head experienced its warmest in 19 years.

Health warnings were issued for vulnerable members of society including babies and young children, the over 65's, those with underlying health conditions, and those who spend a lot of time outdoors. An increase in temperatures typically sees a direct correlation with an increase in hospital admittances, as seen in the 2024 ESRI study. The public were also warned of the risks of sun exposure and the dangers of water-based activities.

A study based on ambient heat in the UK, which has a similar climate to Ireland, found an increased risk of all-cause mortality with increasing temperatures above threshold values

(Arbuthnott & Hajat, 2017). Given these concerning findings, it is important to ascertain to what extent climate change is increasing temperatures nationally.

An understanding of the high temperatures recorded nationally can be better inferred by referring to Figure 1.1. The map shows some of the highest recorded temperatures and their locations for the 11th and 12th of July.

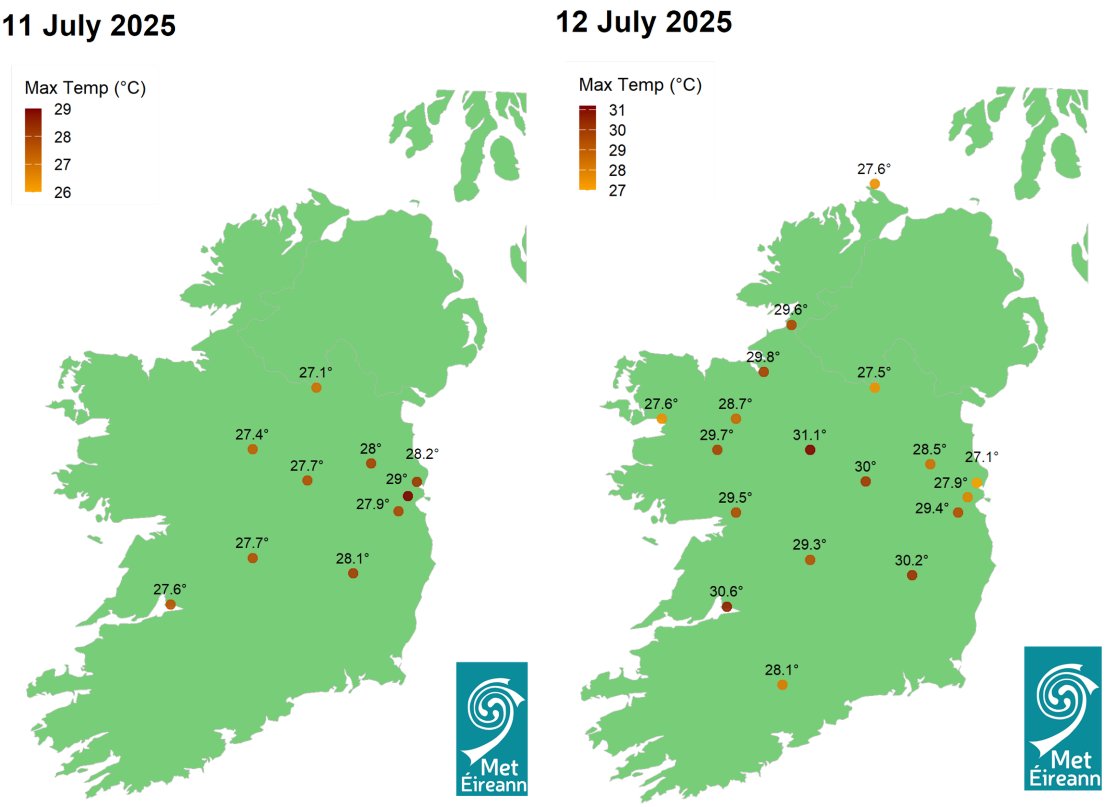

Figure 1.1: Some of the highest recorded temperatures (>27°C) at Met Éireann synoptic stations for the 11th and 12th of July. Highest temperatures were recorded on Saturday the 12th at Mount Dillon (31.1°C), Shannon Airport (30.6°C) and Oak Park (30.2°C).

The synoptic situation (large-scale circulation patterns) leading up to the event was atypical for high-temperature events in Ireland. Ordinarily, such events involve the advection of a warm airmass from the near continent (hot air from Spain, France, Belgium, Netherlands), combined with clear skies, with the resulting solar heating leading to elevated daytime maxima. While continental Europe did experience severe and notable heatwaves leading up to the event there was no warm-air advection from the near continent (i.e. the heat was not imported from these events). Instead, the maxima were primarily the result of in-situ solar heating from a blocking high-pressure system that built over Ireland (Figure 1.2). The system established a slack pressure gradient, allowing for light winds and prolonged sunshine across the country. The event occurred shortly after the summer solstice, a time of high solar insolation and long daylight hours, contributing to elevated surface heating. In addition, antecedent dry conditions (Figure 1.3) may have played a role, reducing soil moisture and limiting evaporatranspiration, which can further amplify surface and near-surface air

temperatures (incoming energy can basically either heat the air or be used to evaporate available water; when there is limited water available more of the energy goes to heating the air). Together, these factors led to a short-lived but intense spell of heat, distinct from the typical synoptic patterns associated with previous extreme temperature events in Ireland.

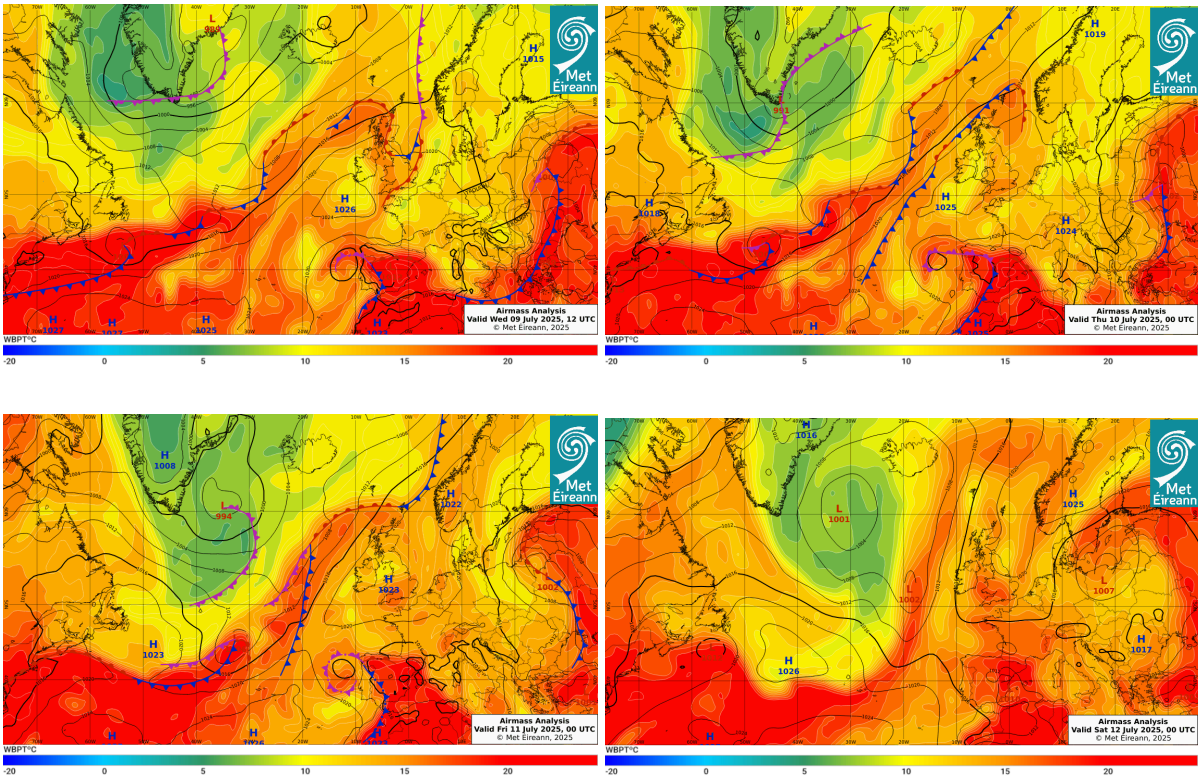

Figure 1.2. Airmass analysis showing the evolution of the synoptic situation leading up to and over the event. Colour scale shows Wet Bulb Potential Temperatures (WBPT, °C) used for identifying temperature contrasts and distinguishing weather features; contours indicate pressure levels (hPa) typical of a synoptic map and H denotes centres of high pressure and L centres of low pressure). Top left: 9th July, top right: 10th July, bottom left: 11th July, and bottom right: 12th July.

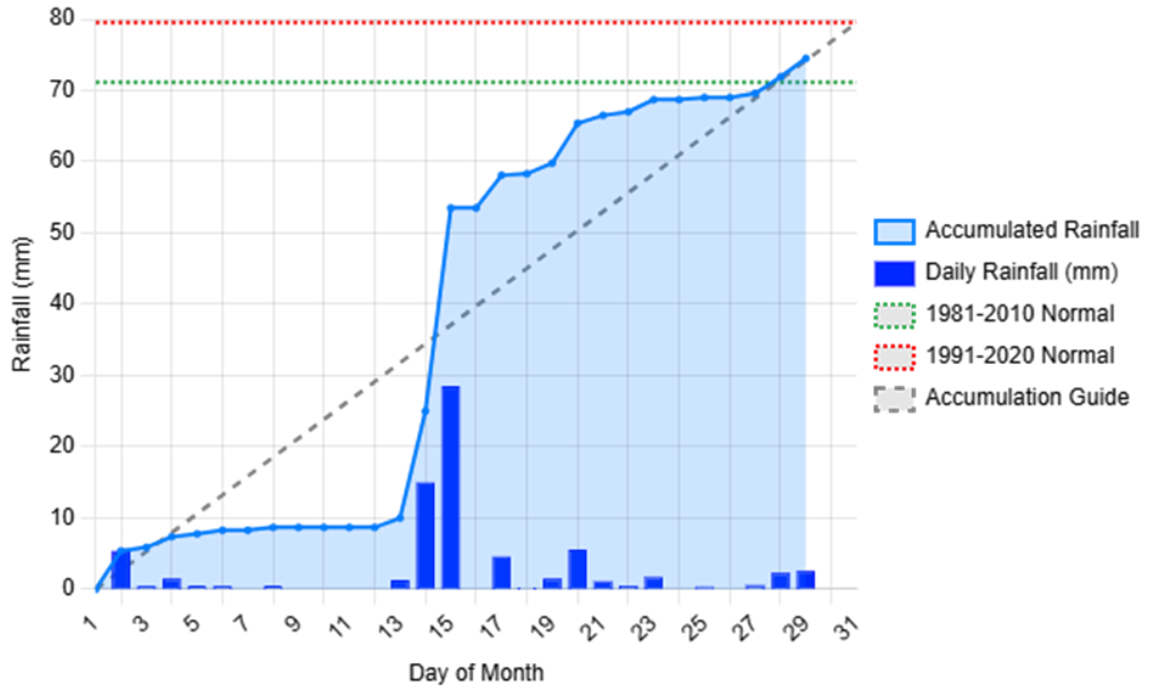

*Figure 1.3. Mullingar rainfall for July 2025, showing below-average rainfall **early in the month** leading up to the hot spell, 11th and 12th of July. The green and red dashed lines indicate the 1981-2010 and 1991-2020 average July rainfall for Mullingar, respectively. Mullingar (County Westmeath) was chosen given its central location in the country as indicative of the broader scale situation.*

1.2 Event Definition

This study examines the abnormally high temperatures of the 11th and 12th of July 2025. Ireland has a similar geographical climatology for summer maximum temperatures throughout the country; therefore, this study looks at mean temperatures over the entire country.

This region also has a strong seasonal cycle in both daily maximum and minimum temperatures (Figure 1.4). There is low variability in these temperatures and a difference of approximately 10°C exists between average winter and summer temperatures.

In this study, we analyse the abnormally hot temperatures using two different metrics:

1. The annual maximum of two-day averaged daily maximum temperatures, Tx2x.
2. The annual maximum of daily maximum temperatures, Tx1x.

Previously, the annual two-day maximum temperature for Ireland has exceeded that of 2025 eight times since Met Éireann records began in 1961 (1976, 1983, 1995, 2006, 2013, 2018, 2021, and 2022). Similarly, the annual one-day maximum temperature for Ireland has exceeded that of 2025 five times in the same record (1983, 2006, 2018, 2021, and 2022). It is noteworthy that 5 of the 8 higher exceedances for a two-day event, and 4 of the 5 higher exceedances for a one-day event, have occurred since 2000 which constitutes roughly the last third of the series.

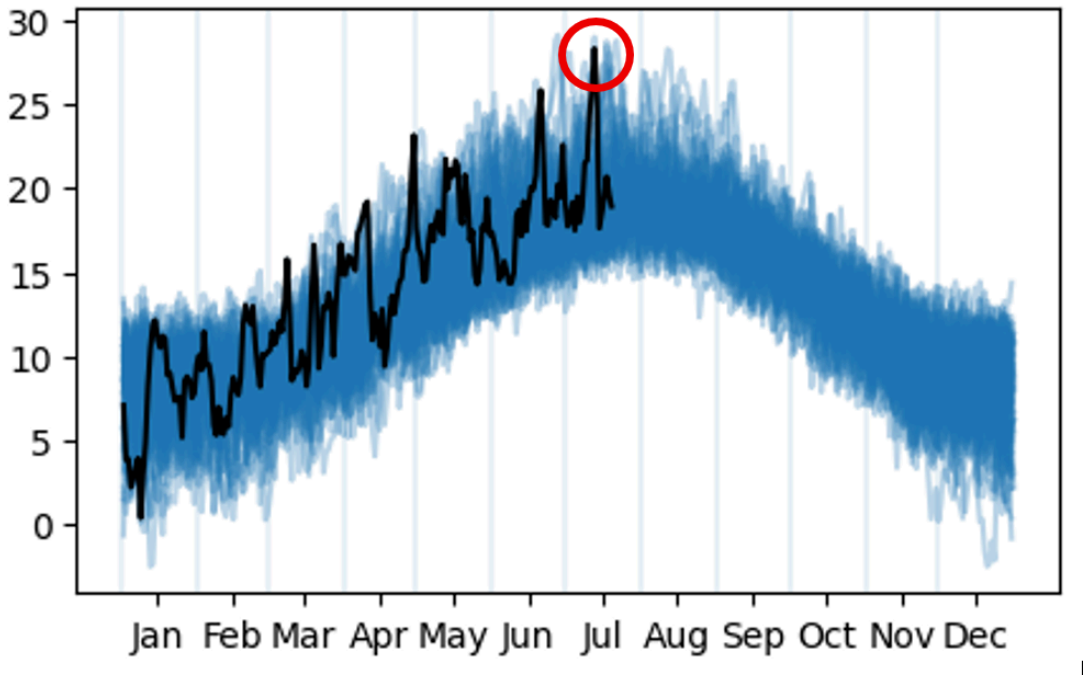

Figure 1.4: Seasonal cycle of two-day average of maximum daily temperatures (Tx2x) averaged over Ireland, from a combination of final and provisional gridded data supplied by Met Éireann, record starts in 1961. The black line shows the present year temperature variation compared with all previous years shown in blue, the event in question is circled in red.

2 Data and methods

2.1 Observational data

Four different gridded observational and reanalysis products were used to analyse this event:

- ERA5: The European Centre for Medium-Range Weather Forecasts' 5th generation reanalysis product, ERA5, is a gridded dataset that combines historical observations into global estimates using advanced modelling and data assimilation systems (Hersbach et al., 2020).
- EOBS: A 0.25° × 0.25° gridded temperature dataset of Europe, formed from the interpolation of station-derived meteorological observations (Cornes et al., 2018).
- CPC: This is the gridded product from NOAA PSL, Boulder, Colorado, USA, available at 0.5° x 0.5° resolution, for the period 1979-present. Data are available from NOAA.
- Met Éireann: The Irish national meteorological services gridded product, from 1961-present, with provisional grids for 2025. Interpolation methods were used to calculate the temperature grid point values with inputs from observations recorded at Met Éireann stations.

Finally, as a measure of anthropogenic climate change, we use the (low-pass filtered) global mean surface temperature (GMST), where GMST is taken from the National Aeronautics

and Space Administration (NASA) Goddard Institute for Space Science (GISS) surface temperature analysis (GISTEMP, Hansen et al., 2010 and Lenssen et al. 2019).

We study the influence of human induced climate change by comparing the likelihood and intensity of similar 2-day and 1-day high temperatures at present with those in a 1.3°C cooler climate. We also extend this analysis into the future by assessing the influence of a further 1.3°C of global warming from present. This is in line with the latest Emissions Gap Report from the United Nations Environment Programme, which shows that the world is on track for at least 2.6 °C temperature rise given currently implemented policies (UNEP, 2024).

2.2 Model and experiment descriptions

We use a multi-model ensemble from climate modelling experiments (Philip et al., 2020). The regional climate models are described as follows:

Coordinated Regional Climate Downscaling Experiment (CORDEX) - European Domain (EURO-CORDEX) with 0.11° resolution (EUR-11) (Jacob et al., 2014; Vautard et al., 2021). The ensemble used here consists of all the regional climate models each of which are driven by a subset of 4 GCMs from the CMIP5 experiment. These simulations are composed of historical simulations up to 2005 and extended to the year 2100 using the RCP8.5 scenario.

2.3 Statistical methods

The methods for observational and model analysis, and for model evaluation and synthesis, follow the World Weather Attribution Protocol, described in Philip et al., (2020), with supporting details found in van Oldenborgh et al., (2021), Ciavarella et al., (2021) and WWA, 2021. The key steps, presented in sections 3-6, are: (3) trend estimation from observations; (4) model evaluation; (5) multi-method multi-model attribution; and (6) synthesis of the attribution statement. In addition, section 7 presents the societal impacts of the extreme weather event and section 8 gives a brief conclusion.

We calculate the return periods, Probability Ratio (PR; the factor-change in the event's probability) and change in intensity of the event under study to compare the climate of now and the climate of the past, defined respectively by the GMST values of now and of the preindustrial past (1850-1900, based on the Global Warming Index).

To statistically model the unusual one-day and two-day high temperatures, we use a nonstationary generalised extreme value (GEV) distribution. The distribution is assumed to shift linearly with the covariates, while the variance remains constant. Next, results from observations and models that pass the validation tests are synthesised to produce a single attribution statement.

3 Observational analyses: return period and trend

In this section, trends in observational datasets (the gridded data products set out in section 2.1) are calculated and compared. We analyse the area average Tx2x and Tx1x for all four gridded datasets and calculate the return period, change in intensity and probability ratio

(along with the 95% confidence interval) between the current climate of 2025 and a past climate, that is 1.3°C cooler, by fitting the data to a nonstationary generalised extreme value (GEV) distribution.

Evaluating the four different observation-based gridded datasets, there is no evidence to suggest they are misrepresenting the observed station data in either trend or variability. Therefore, all four gridded datasets are used.

As mentioned previously, this was not the warmest 2-day period previously recorded in Ireland. However, the regularity of a 2-day high temperature event is increasing for the country and so was chosen for this study. Given that July is one of the warmest months in general for Ireland, the analysis was carried out for all twelve months of the year. Thus, the analysis represents the annual 2-day and 1-day maximum temperatures experienced in Ireland.

At the time of writing, only three of the four observation-based datasets include the event (Met Éireann, CPC and ERA5), and one of these is as a forecast (ERA5). We therefore first use these three datasets to estimate the return period of the extreme heat over the study region. Focusing on the three datasets that record the event, Met Éireann and CPC both almost agree when calculating the best estimates of the probability ratio, ERA5 estimates a slightly larger value but, as mentioned, this is based on forecasted data. Given the results from these three observation-based datasets, and putting more faith in the Met Éireann and CPC data, we consider changes in the 1-in-6-year event for Tx2x and the 1-in-8-year event for Tx1x. These values are then used for the EOBS data.

For each event definition, the results of trend fitting are presented in tables (Tables 3.1 – 3.2). An illustration of the calculated trend and statistical fit are also displayed, using the Met Éireann dataset as an example (Figures 3.1 – 3.2).

3.1 Tx2x

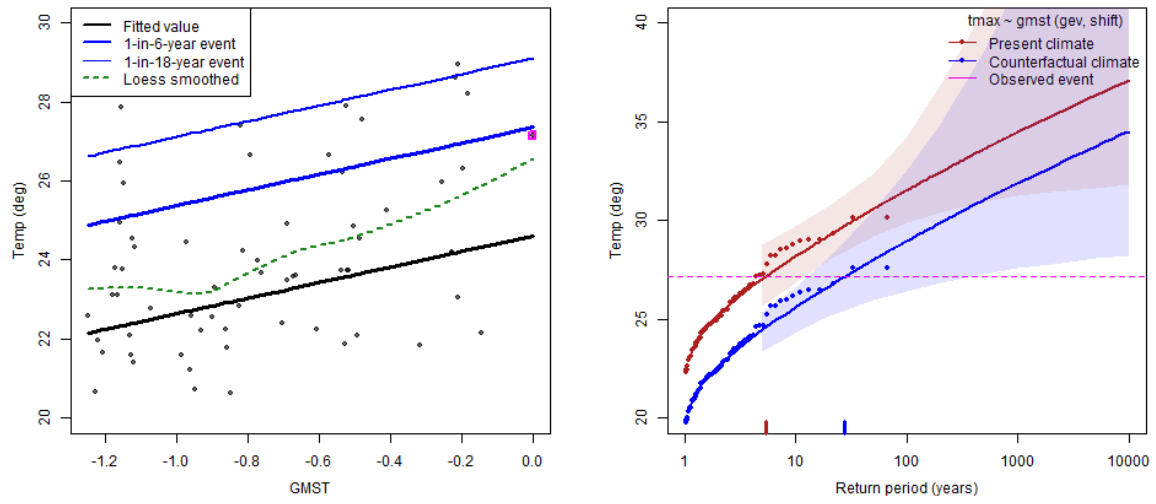

Figure 3.1: The 2-day high temperature event from 1961-present from the Met Éireann dataset. Left: the observed distribution scaling with the covariate GMST and resultant trend. The 2025 event is

highlighted in the pink box. Right: return periods of events if they occurred in 2025 (red) or in a 1.3°C cooler world (blue). The 2025 event magnitude is highlighted by the pink horizontal dashed line.

Tx2x	Event		GMST trend	
Dataset	Magnitude (°C)	Return period (95% C.I.)	Probability ratio (95% C.I.)	Change in intensity (°C) (95% C.I.)
ERA5	25.95	9.53	**3.465 (1.191 – 25.966)**	**1.625 (0.226 – 3.223)**
Met Eireann	27.16	5.34	**5.16 (1.595 – 128.789)**	**2.574 (0.918 – 5.029)**
CPC	27.10	6.08	**10.666 (1.412 – Inf)**	**3.132 (0.609 – 6.392)**
EOBS	26.14	6.00	1.788 (0.879 – 5.691)	0.963 (-0.231 – 2.512)

Table 3.1: Results from trend analysis of the 2-day high temperature event. Return period and magnitudes as observed in Met Éireann and CPC, forecasted for ERA5, and magnitudes of the 1-in-6-year high temperature event in the EOBS dataset in 2024 for the region over Ireland. Statistically significant results are in bold. The value Inf implies that the upper bound is unbounded (infinity) for CPC probability ratio which implies the event may not have been possible in this particular product in the pre-industrial world. Orange shading represents the 2-day *high temperature event.*

3.2 Tx1x

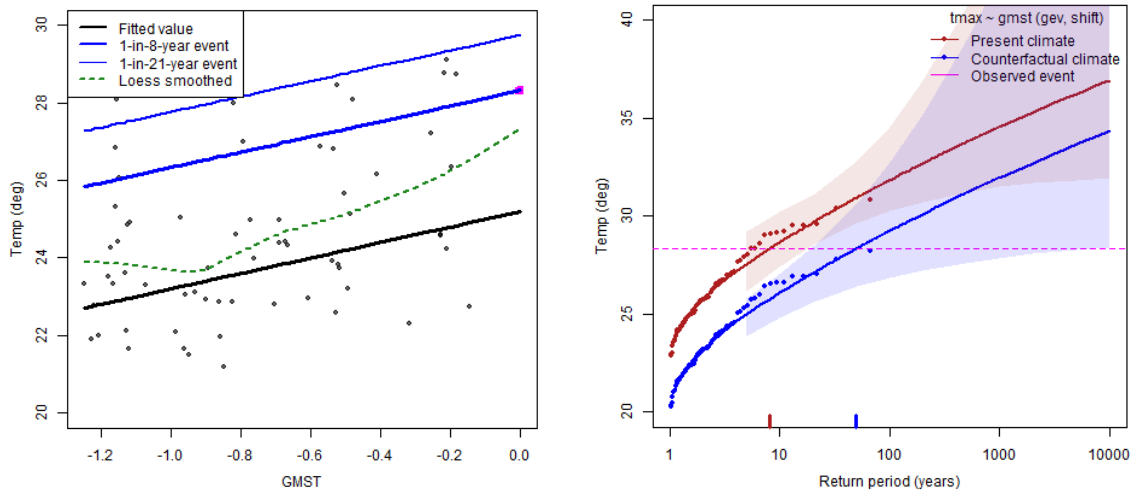

Figure 3.2: The 1-day high temperature event from 1961-present from the Met Éireann dataset. Left: the observed distribution scaling with the covariate GMST and resultant trend. The 2025 event is highlighted in the pink box. Right: return periods of events if they occurred in 2025 (red) or in a 1.3°C cooler world (blue). The 2025 event magnitude is highlighted by the pink line.

Tx1x	Event		GMST trend	
Dataset	Magnitude (°C)	Return period (95% C.I.)	Probability ratio (95% C.I.)	Change in intensity (°C) (95% C.I.)
ERA5	26.78	11.63	**4.01 (1.15 – 78.39)**	**1.73 (0.15 – 3.47)**
Met Eireann	28.32	7.98	**6.1 (1.61 – 855.40)**	**2.59 (0.98 – 5.00)**
CPC	28.42	7.59	**4.13 (1.39 - Inf)**	**2.99 (0.90 – 6.33)**
EOBS	27.07	8.00	1.64 (0.86 – 4.31)	0.83 (-0.25 – 2.09)

Table 3.2 Results from trend analysis of the 1-day high temperature event. Return period and magnitudes as observed in Met Éireann and CPC, forecasted for ERA5, and magnitudes of the 1-in-8-year high temperature event in the EOBS dataset in 2024 for the region over Ireland. Statistically significant results are in bold. The value Inf implies that the upper bound is unbounded (infinity) for CPC probability ratio which implies the event may not have been possible in this particular product in the pre-industrial world. Red shading represents the 1-day *high temperature event.*

4 Model evaluation

In the subsections below we show the results of the model evaluation. The climate models are evaluated against the observations in their ability to capture:

1. Seasonal cycles: For this, we qualitatively compare the seasonal cycles in model outputs against observations-based cycles. We discard the models that exhibit ill-defined peaks in their seasonal cycles.
2. Spatial patterns: Models that do not match the observations in terms of the large-scale temperature patterns are excluded.
3. Parameters of the fitted statistical models: The statistical fit parameters must lie within the equivalent observational parameter uncertainty range (good), or their uncertainty ranges must overlap (reasonable).

The models are labelled as ‘good’, ‘reasonable’, or ‘bad’ based on their performances in terms of the three criteria discussed above. A model is given an overall rating of ‘good’ if it is rated ‘good’ for all characteristics. If there is at least one ‘reasonable’ the overall rating is ‘reasonable’, and if there is at least one ‘bad’ the overall rating is ‘bad’. Only models that are labelled as ‘good’ overall are used in the final analysis.

From the CORDEX ensemble, 20 good models are used for Tx2x, and 22 good models are used for Tx1x. Tables showing how the respective models chosen are shown in A.1 and A.2 in the appendix. Visuals for choosing the seasonal cycles and spatial patterns are shown in A.3 and A.4 respectively.

5 Multi-method multi-model attribution

Before any synthesis of the models can be carried out, the models that passed the evaluation in section 4 must be gathered and their results combined for the synthesis outlined in section 6. Tables 5.1 and 5.2 below show the probability ratios and changes in intensity ΔI for models that passed model evaluation, alongside those from observational data products. This is calculated for both past to present and present to future.

5.1 Tx2x

		Preindustrial - Present (1.3 ˚C)		Present - Future (2.6 ˚C)	
Model / Observations	Threshold return period	Probability ratio PR [-]	Change in intensity ΔI [%]	Probability ratio PR [-]	Change in intensity ΔI [%]
cpc	27.1˚C	10.67 (1.41…Inf)	3.13 (0.61…6.39)		
EOBS	26.14˚C	1.79 (0.88…5.69)	0.96 (-0.23…2.51)		
era5	25.95˚C	3.46 (1.19…25.97)	1.63 (0.23…3.22)		
MEgrid	27.16˚C	5.16 (1.6…128.79)	2.57 (0.92…5.03)		
EC-EARTH_r12_CCLM4-8-17	20.99˚C	1.67 (1.55…2.38)	0.75 (0.57…1)	2.02 (1.76…2.44)	1.14 (0.89…1.46)
EC-EARTH_r12_REMO2015	21.56˚C	3.52 (1.78…27.33)	1.33 (0.64…2.03)	2.32 (1.9…2.69)	1.2 (0.87…1.38)
EC-EARTH_r12_WRF381P	21.41˚C	2.08 (1.6…8.12)	1.32 (0.92…2.84)	2.06 (1.81…2.91)	1.34 (1.12…1.81)
EC-EARTH_r3_COSMO-crCLIM-v1-1	20.95˚C	4.05 (1…Inf)	1.25 (-0.06…1.74)	2.6 (2.36…3.53)	1.24 (1.04…1.58)
HadGEM2-ES_r1_ALADIN63	23.58˚C	2.93 (1.62…3.51)	1.78 (0.78…2.57)	2.35 (2.22…2.68)	1.69 (1.62…2.03)
HadGEM2-ES_r1_HadREM3-GA7-05	23.22˚C	2.93 (1.84…12.24)	1.71 (1.01…2.56)	2.89 (2.59…3.57)	1.98 (1.72…2.23)
HadGEM2-ES_r1_HIRHAM5	22.78˚C	3.59 (2…6.64)	1.67 (0.84…2.31)	2.87 (2.74…3.33)	1.69 (1.6…1.92)
HadGEM2-ES_r1_RACMO22E	22.42˚C	1.89 (1.39…2.49)	1.31 (0.75…2.13)	2.26 (2.03…2.47)	1.64 (1.46…1.83)
HadGEM2-ES_r1_RCA4	22.51˚C	3.09 (1.86…3.46)	1.8 (1.03…1.84)	2.47 (2.36…2.64)	1.72 (1.6…1.83)
HadGEM2-ES_r1_WRF361H	22.23˚C	2.26 (1.9…4.52)	1.41 (1.07…1.68)	2.46 (2.13…2.73)	1.67 (1.35…1.68)
HadGEM2-ES_r1_WRF381P	22.79˚C	1.77 (1.46…1.86)	1.39 (0.89…2.02)	1.97 (1.92…2.16)	1.53 (1.42…1.85)
MPI-ESM-LR_r1_ALADIN63	22.22˚C	2.07 (1.65…2.82)	1.34 (0.94…2.38)	2.05 (1.74…2.98)	1.6 (1.28…2.24)
MPI-ESM-LR_r1_COSMO-crCLIM-v1-1	21.64˚C	2.01 (0.99…2.24)	0.87 (-0.02…0.92)	1.8 (1.63…2.24)	0.95 (0.79…1.2)
MPI-ESM-LR_r1_HadREM3-GA7-05	21.49˚C	2.47 (1.94…3.47)	1.38 (1.03…1.94)	2.04 (1.94…2.59)	1.4 (1.26…1.85)
MPI-ESM-LR_r1_RegCM4-6	21.34˚C	2.04 (1.27…4.05)	1.3 (0.49…2.22)	1.82 (1.62…1.99)	1.12 (0.91…1.5)
MPI-ESM-LR_r2_REMO2009	21.12˚C	1.49 (0.92…2.28)	0.63 (-0.18…1.17)	2.01 (1.62…2.47)	1.15 (0.61…1.54)

MPI-ESM-LR_r3_COSMO-crCLIM-v1-1	21.46˚C	3.18 (2.45…10.2)	1.23 (0.85…2.43)	2.31 (1.88…2.91)	1.17 (0.86…1.52)
MPI-ESM-LR_r3_REMO2015	21.47˚C	1.84 (1.64…5.1)	0.93 (0.73…2.53)	1.99 (1.73…2.54)	1.11 (0.89…1.52)
NorESM1-M_r1_COSMO-crCLIM-v1-1	21.28˚C	5.07 (1.73…40.56)	1.33 (0.56…1.83)	2.7 (2.43…3.03)	1.23 (1.12…1.45)
NorESM1-M_r1_REMO2015	21.63˚C	4.33 (1.47…6.77)	1.69 (0.61…2.04)	2.37 (2.12…2.67)	1.3 (1.2…1.46)

Table 5.1: Event magnitude, probability ratio and change in intensity for 6-year return period for Tx2x for observational datasets and each model that passed the evaluation tests. (a) from pre-industrial climate to the present and (b) from the present to 2.6 °C above pre-industrial climate.

5.2 Tx1x

		Preindustrial - Present (1.3 ˚C)		Present - Future (2.6 ˚C)	
Model / Observations	**Threshold return period**	**Probability ratio PR [-]**	**Change in intensity ΔI [%]**	**Probability ratio PR [-]**	**Change in intensity ΔI [%]**
cpc	28.42˚C	4.14 (1.39…Inf)	2.99 (0.9…6.33)		
EOBS	27.07˚C	1.64 (0.86…4.31)	0.83 (-0.25…2.09)		
era5	26.77˚C	4.01 (1.15…78.39)	1.73 (0.15…3.47)		
MEgrid	28.32˚C	6.1 (1.61…855.4)	2.59 (0.98…5)		
EC-EARTH_r1_COSMO-crCLIM-v1-1	21.14˚C	5.1 (4.52…253.75)	1.71 (1.32…2.43)	2.41 (1.76…3.08)	1.08 (0.69…1.24)
EC-EARTH_r12_CCLM4-8-17	21.41˚C	1.69 (1.58…2.54)	0.75 (0.57…1)	2.11 (1.82…2.69)	1.14 (0.89…1.46)
EC-EARTH_r12_REMO2015	21.91˚C	3.93 (1.86…51.34)	1.33 (0.64…2.03)	2.53 (2…2.98)	1.2 (0.87…1.38)
EC-EARTH_r12_WRF381P	21.93˚C	2.08 (1.57…9.22)	1.32 (0.92…2.84)	2.11 (1.83…3.21)	1.34 (1.12…1.81)
EC-EARTH_r3_COSMO-crCLIM-v1-1	21.26˚C	4.69 (1.01…Inf)	1.25 (-0.06…1.74)	2.88 (2.59…4.25)	1.24 (1.04…1.58)
HadGEM2-ES_r1_ALADIN63	24.09˚C	3.06 (1.63…3.44)	1.78 (0.78…2.57)	2.51 (2.33…2.87)	1.69 (1.62…2.03)
HadGEM2-ES_r1_HadREM3-GA7-05	23.69˚C	3.01 (1.87…16.73)	1.71 (1.01…2.56)	3.14 (2.78…4.12)	1.98 (1.72…2.23)
HadGEM2-ES_r1_HIRHAM5	23.19˚C	3.8 (2.13…7.76)	1.67 (0.84…2.31)	3.18 (3.08…3.72)	1.69 (1.6…1.92)

HadGEM2-ES_r1_RACMO22E	23.01˚C	1.89 (1.38…2.39)	1.31 (0.75…2.13)	2.37 (2.07…2.63)	1.64 (1.46…1.83)
HadGEM2-ES_r1_RCA4	22.97˚C	3.11 (1.86…3.59)	1.8 (1.03…1.84)	2.59 (2.43…2.87)	1.72 (1.6…1.83)
HadGEM2-ES_r1_WRF361H	22.73˚C	2.27 (1.89…4.89)	1.41 (1.07…1.68)	2.63 (2.27…2.98)	1.67 (1.35…1.68)
HadGEM2-ES_r1_WRF381P	23.48˚C	1.76 (1.46…1.8)	1.39 (0.89…2.02)	2 (1.91…2.18)	1.53 (1.42…1.85)
MPI-ESM-LR_r1_ALADIN63	22.77˚C	2.14 (1.68…2.81)	1.34 (0.94…2.38)	2.17 (1.79…3.37)	1.6 (1.28…2.24)
MPI-ESM-LR_r1_COSMO-crCLIM-v1-1	22.02˚C	2.15 (0.99…2.63)	0.87 (-0.02…0.92)	1.92 (1.7…2.52)	0.95 (0.79…1.2)
MPI-ESM-LR_r1_HadREM3-GA7-05	21.95˚C	2.57 (1.99…3.75)	1.38 (1.03…1.94)	2.15 (2.04…2.86)	1.4 (1.26…1.85)
MPI-ESM-LR_r1_RegCM4-6	21.86˚C	2.02 (1.27…4)	1.3 (0.49…2.22)	1.85 (1.65…2.03)	1.12 (0.91…1.5)
MPI-ESM-LR_r2_REMO2009	21.58˚C	1.52 (0.92…2.36)	0.63 (-0.18…1.17)	2.13 (1.73…2.69)	1.15 (0.61…1.54)
MPI-ESM-LR_r3_COSMO-crCLIM-v1-1	21.8˚C	3.48 (2.67…12.98)	1.23 (0.85…2.43)	2.53 (2…3.24)	1.17 (0.86…1.52)
MPI-ESM-LR_r3_REMO2015	21.92˚C	1.89 (1.7…5.45)	0.93 (0.73…2.53)	2.14 (1.82…2.78)	1.11 (0.89…1.52)
NorESM1-M_r1_COSMO-crCLIM-v1-1	21.56˚C	5.94 (1.81…98.25)	1.33 (0.56…1.83)	2.98 (2.64…3.37)	1.23 (1.12…1.45)
NorESM1-M_r1_RegCM4-6	21.3˚C	7.35 (5.35…Inf)	1.79 (0.92…2.21)	3.61 (3.54…4.43)	1.48 (1.33…1.76)
NorESM1-M_r1_REMO2015	22˚C	4.74 (1.48…7.52)	1.69 (0.61…2.04)	2.52 (2.24…2.84)	1.3 (1.2…1.46)

Table 5.2: Event magnitude, probability ratio and change in intensity for 8-year return period for Tx1x for observational datasets and each model that passed the evaluation tests. (a) from pre-industrial climate to the present and (b) from the present to 2.6 °C above pre-industrial climate.

6 Hazard synthesis

For the event definitions described above we evaluate the influence of anthropogenic climate change on the events by calculating the probability ratio as well as the change in intensity using observations and climate models. Models which do not pass the evaluation described above are excluded from the analysis. The aim is to synthesise results from models that pass the evaluation, along with the observation-based products, to give an overarching attribution statement.

Figures 6.1-6.4 show the changes in probability and intensity for the observations (blue) and models (red). Before combining them into a synthesised assessment, first, a representation error is added (in quadrature) to the observations, to account for the difference between observations-based datasets that cannot be explained by natural variability. This is shown in these figures as white boxes around the light blue bars. The dark blue bar shows the average over the observation-based products. Next, a term to account for intermodel spread is added (in quadrature) to the natural variability of the models. This is shown in the figures as white boxes around the light red bars. The dark red bar shows the model average, consisting of a weighted mean using the (uncorrelated) uncertainties due to natural variability plus the term representing intermodel spread (i.e., the inverse square of the white bars).

Observation-based products and models are combined into a single result in two ways. Firstly, we neglect common model uncertainties beyond the intermodel spread that is depicted by the model average and compute the weighted average of models (dark red bar) and observations (dark blue bar): this is indicated by the magenta bar. As, due to common model uncertainties, model uncertainty can be larger than the intermodel spread, secondly, we also show the more conservative estimate of an unweighted, direct average of observations (dark blue bar) and models (dark red bar) contributing 50% each, indicated by the white box around the magenta bar in the synthesis figures.

Results are shown in Table 6.1, where differences are presented for changes both between the past, 1.3°C cooler climate, and today's climate, and between the present and a future, 1.3°C warmer climate. By combining evidence from the synthesis of model results for the past, projections for the future, and established physical understanding, we derive a best-estimate attribution of the event.

We conclude a probability ratio of about 2.3 for Tx2x and 2.6 for Tx1x, and note that these trends continue into the future, with a probability ratio of another 2.3 times for Tx2x and another 2.5 times for Tx1x. That is to say that the 2-day event has already been made 2.3 times more likely and the one-day event 2.6 times more likely due to climate change. These increases in likelihood will continue into the future. The intensity changes between past and present for Tx2x is about 1.3°C, and for Tx1x this is about 1.4°C. This continues into the future with another approximate 1.4°C change for both Tx2x and Tx1x in a world that has warmed by an additional 1.3°C. We note that the model results overall suggest weaker increases in both probability and intensity than the observationally based estimates for the historical period. The final estimates are dominated by the model estimates given their much smaller uncertainties. It is possible that models may have systematically underestimated the changes and thus the results presented here both for historical changes and future projections are conservative estimates. Prior studies, as assessed in IPCC AR6 generally show the greatest increases in intensity and probability for the truly extreme-tail extremes with more modest changes for more frequent extremes such as those studied here. The results here are in-line with this.

Data		Tx2x		Tx1x	
		Probability ratio (95% CI)	Intensity change [°C] (95% CI)	Probability ratio (95% CI)	Intensity change [°C] (95% CI)
Observations	Past-Present	4.297 (0.629 to 135.148)	2.074 (-0.467 to 4.989)	3.588 (0.773 – 90.399)	2.036 (-0.430 – 4.924)
Models		**2.209 (1.281 to 4.420)**	**1.279 (0.531 to 2.035)**	**2.500 (1.055 – 7.915)**	**1.326 (0.556 – 2.103)**
Synthesis		**2.285 (1.152 to 6.387)**	**1.335 (0.347 to 2.398)**	2.641 (0.977 – 13.694)	**1.381 (0.373 – 2.476)**
Models Only	Present-Future	**2.260 (1.727 to 3.065)**	**1.405 (0.878 to 1.975)**	**2.454 (1.739 – 3.606)**	**1.395 (0.869 – 1.958)**

Table 6.1: Summary of results for Tx2x (left) and Tx1x (right), presented in Figs 6.1-6.4: changes due to GMST include past-present changes and present-future. Statistically significant values are in bold. Orange shading represents the 2-day *high temperature event and red* shading represents the 1-day *high temperature event.*

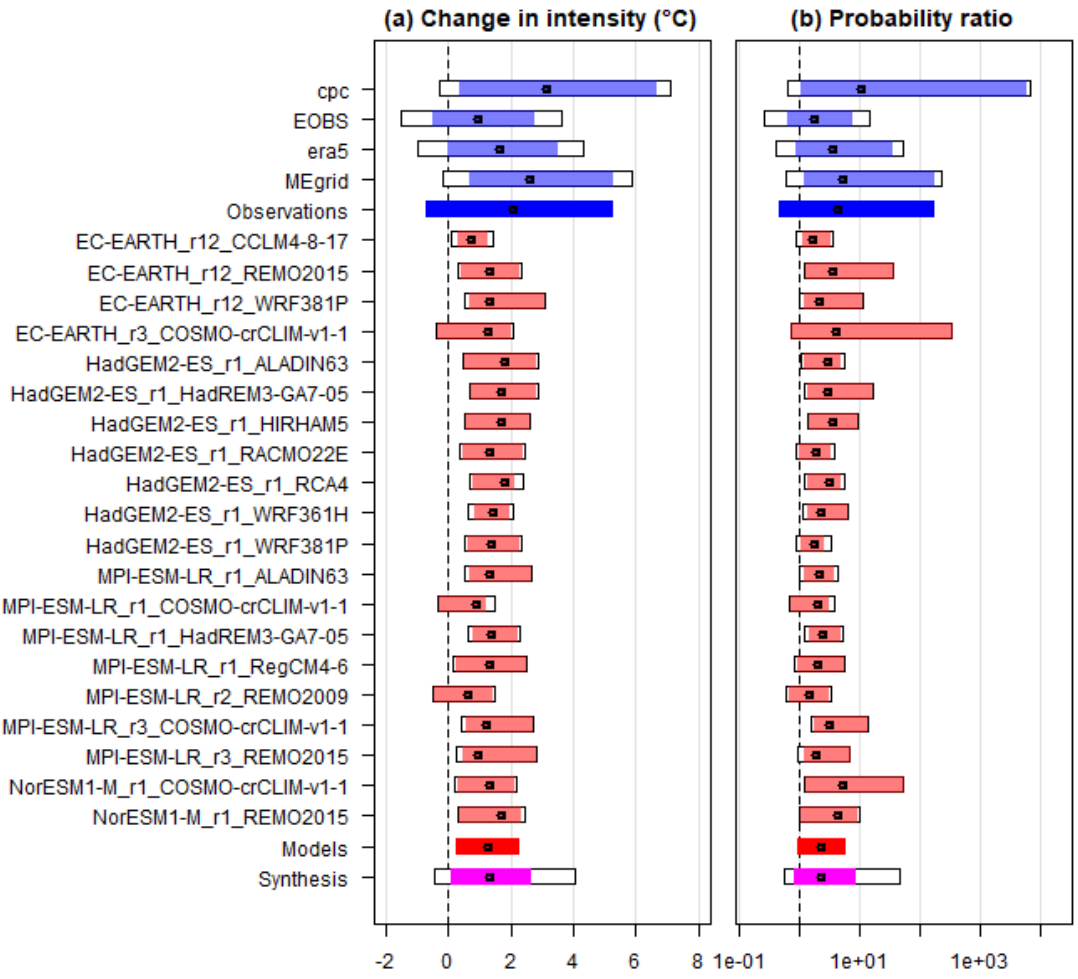

Figure 6.1: Synthesised changes for a 6-year Tx2x event due to GMST. Changes in intensity (left) and PR (right) are shown for a historical period comparing the past 1.3°C cooler climate with the present.

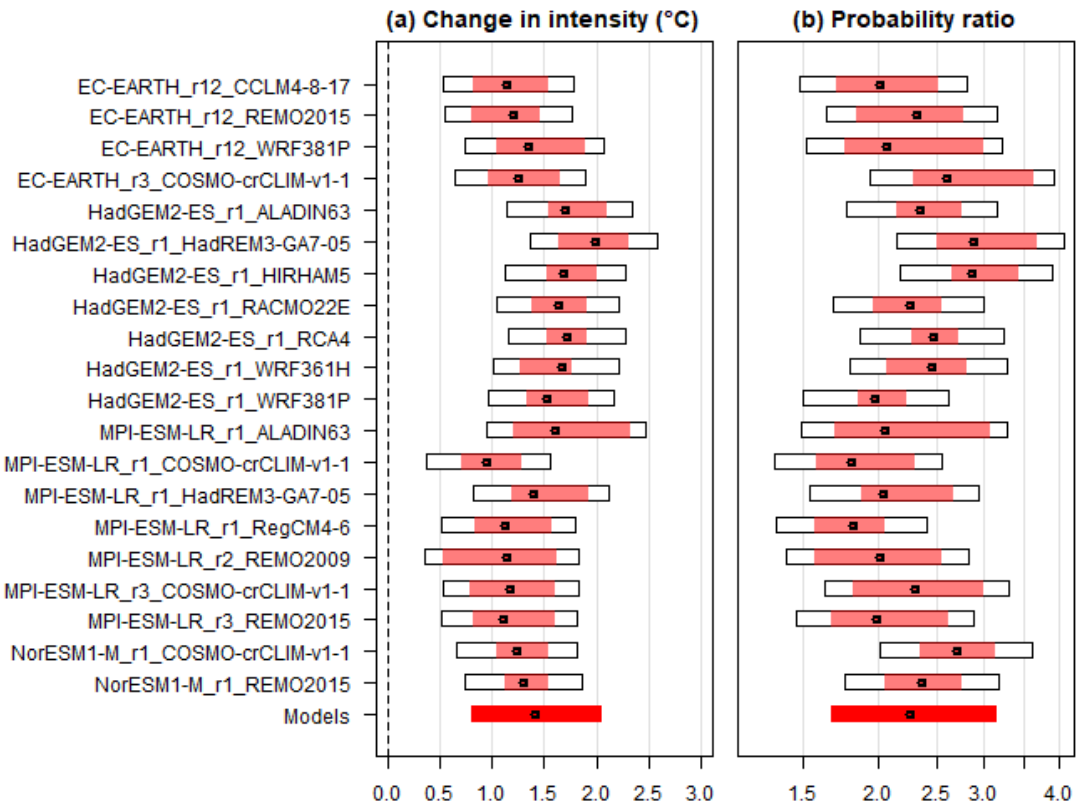

Figure 6.2: Synthesised changes for a 6-year Tx2x event due to GMST. Changes in intensity (left) and PR (right) are shown for a future period, based on model projections only, comparing the present and a 2.6 °C warmed climate (a further 1.3 °C above present).

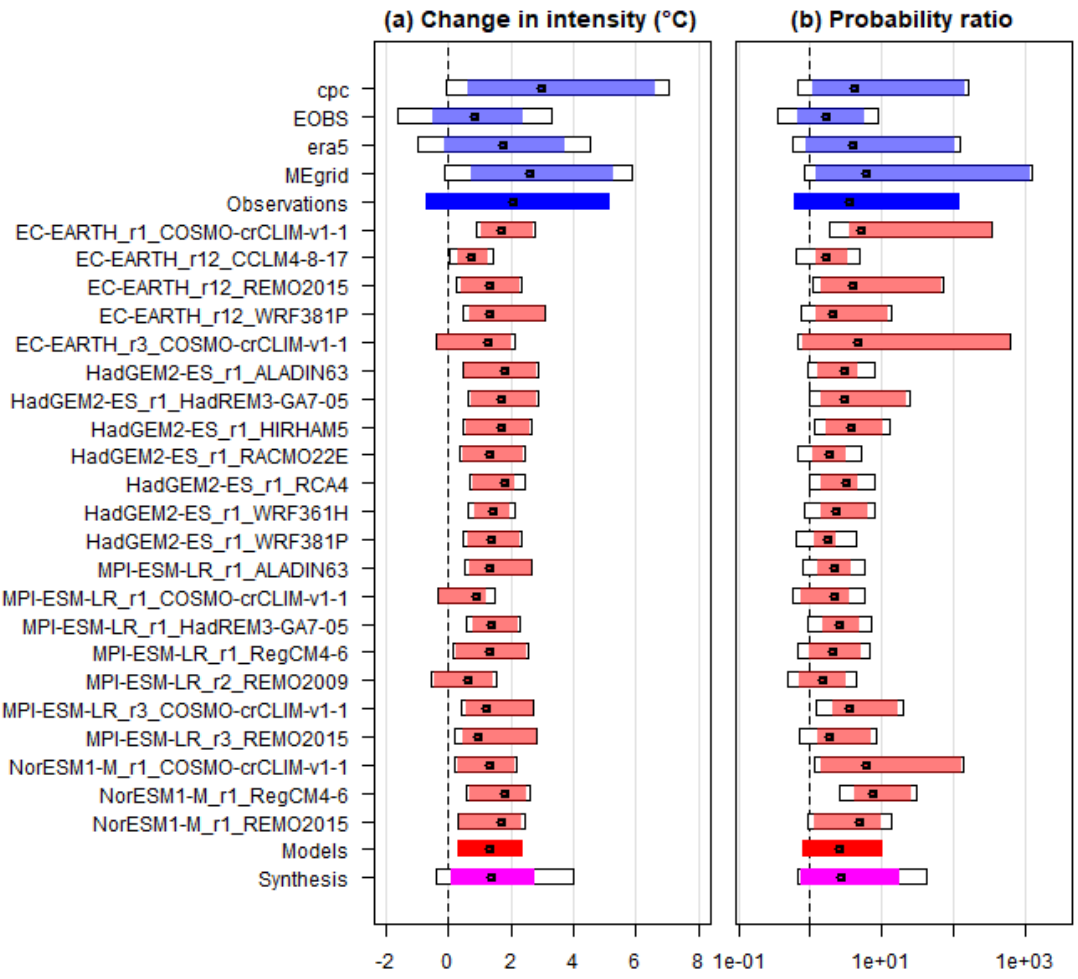

Figure 6.3: Synthesised changes for an 8-year Tx1x event due to GMST. Changes in intensity (left) and PR (right) are shown for a historical period comparing the past 1.3°C cooler climate with the present.

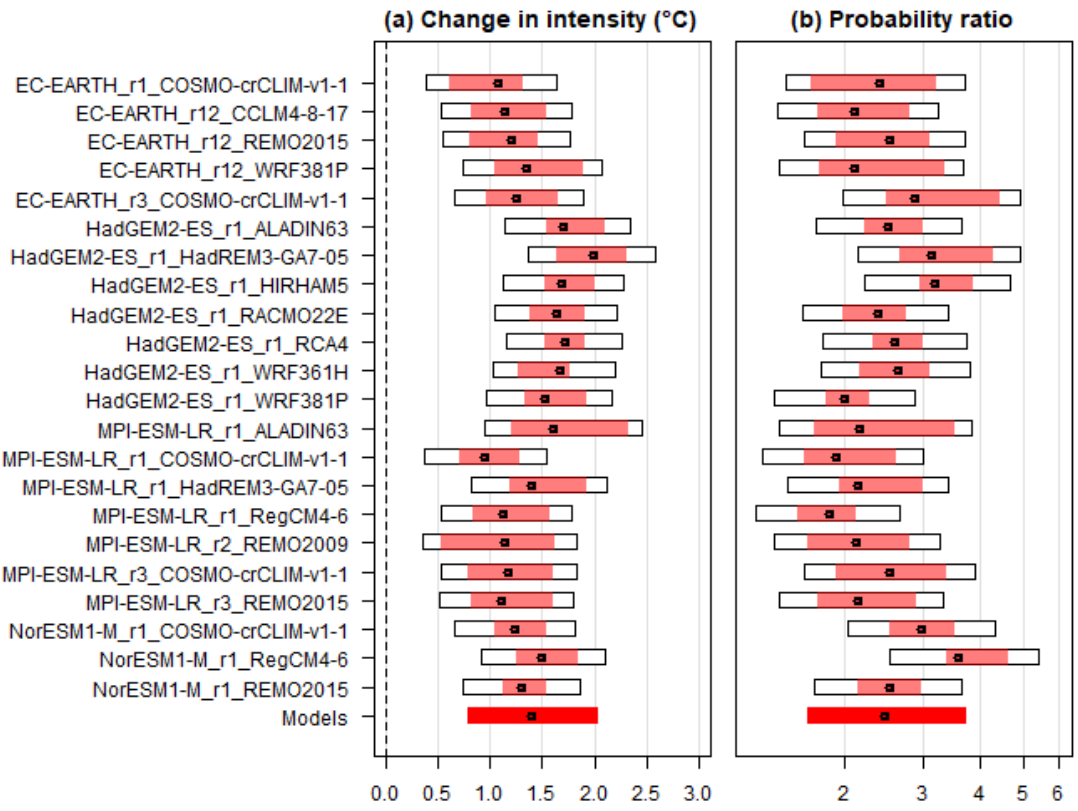

Figure 6.4: Synthesised changes for an 8-year Tx2x event due to GMST. Changes in intensity (left) and PR (right) are shown for a future period, based on model projections only, comparing the present and a 2.6 °C warmed climate (a further 1.3 °C above present).

7 Societal impacts

In addition to the high temperatures recorded during the day, the map in Figure 7.1 shows some of the high nighttime maxima for the night of the 11th to 12th of July. When higher than average temperatures persist through the night the body is unable to rest and recover from the day's heat.

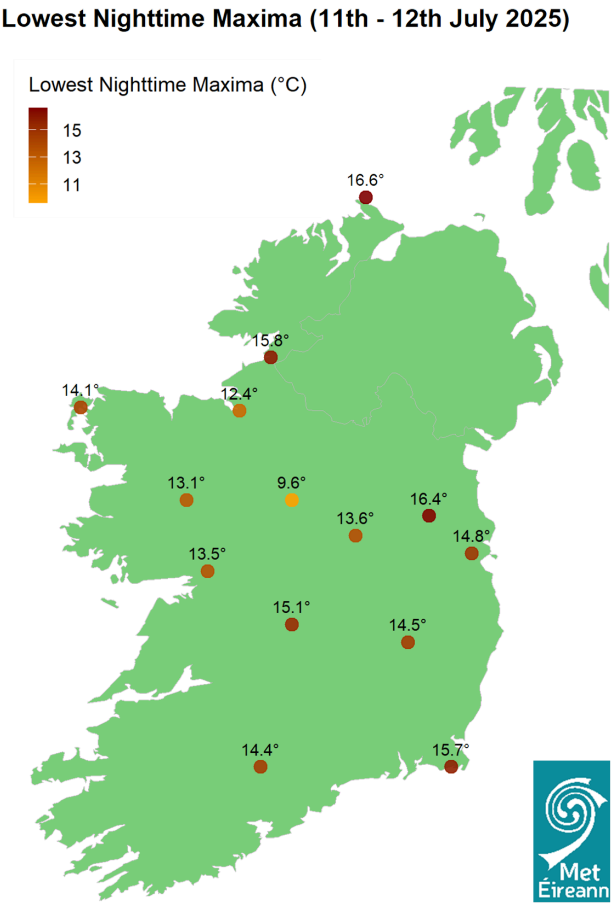

Figure 7.1: Some of the lowest recorded temperatures at Met Éireann synoptic stations for the high nighttime maxima from 21 UTC on the 11th to 09 UTC on the 12th of July. Highest nighttime maxima were recorded at Malin Head (16.6°C), Dunsany (16.4°C) and Finner (15.8°C).

The increased heat can also have a number of additional adverse effects. With warm and dry conditions leading up to the weekend of the 11th to 12th of July, the Department of Agriculture issued a red level forest fire warning for the weekend. A red level warning is the highest warning issued by the department and its issuance is rare. So far this year, over 4,300 hectares of land had already been affected by wildfires, with seven previous fire warnings being issued due to high-risk weather.

The previously warm and dry spring had led to a struggling water supply, with hosepipe bans ongoing for a number of weeks at three different locations in Ireland (Mullingar, Co Westmeath, Milford, Co Donegal and Kells-Oldcastle in Co Meath.). The high temperatures of this weekend added additional strain to the water supply.

In addition, warm temperatures in Ireland tend to see an increase in visitors at beaches and large bodies of water. With this comes an increase in injuries and fatalities due to water-based accidents. Sadly one death did occur over this two day period, where a young girl drowned while swimming.

As well as leading to an increase in leisure based accidents, high temperatures at the start of the weekend caused an area of road in Co. Cork to melt. Motorists were told to avoid the area until temperatures dropped and the tar set again, as the road was impassable in the heat.

8 Conclusion

Overall, we conclude that both two-day (11^{th}-12^{th} July) and one-day (12^{th} July) high temperature periods respectively are more likely than they would have been without climate change. The two-day high temperatures observed this year have already been made 2.3 times as likely, while the one-day high temperatures have been made 2.6 times as likely. Both events are approximately 1.3°C hotter than would have been the case in the pre-industrial climate because of human induced climate change.

References

All references are given as hyperlinks in the text.

Appendix

Model / Observations	Seasonal cycle	Spatial pattern	Sigma	Shape	Summary
cpc			1.73 (1.27…2.13)	0 (0…0)	
EOBS			1.68 (1.41…1.94)	-0.04 (-0.23…0.11)	
era5			1.56 (1.27…1.85)	-0.07 (-0.25…0.1)	
MEgrid			1.68 (1.31…2.02)	-0.05 (-0.28…0.17)	
CNRM-CM5_r1_ALADIN63	reasonable	good	1.64 (1.44…1.79)	-0.05 (-0.09…-0.01)	reasonable
CNRM-CM5_r1_CCLM4-8-17	reasonable	good	1.87 (1.58…1.95)	-0.15 (-0.25…0.07)	reasonable
CNRM-CM5_r1_HadREM3-GA7-05	reasonable	good	1.6 (1.43…1.63)	-0.14 (-0.17…0.02)	reasonable
CNRM-CM5_r1_HIRHAM5	reasonable	good	1.39 (1.16…1.64)	-0.27 (-0.5…-0.08)	reasonable
CNRM-CM5_r1_RACMO22E	reasonable	reasonable	1.65 (1.4…1.69)	-0.18 (-0.22…0.03)	reasonable
CNRM-CM5_r1_RCA4	reasonable	good	1.45 (1.18…1.41)	-0.08 (-0.15…-0.02)	reasonable
CNRM-CM5_r1_REMO2015	reasonable	good	1.6 (1.28…1.92)	-0.19 (-0.44…0.01)	reasonable
CNRM-CM5_r1_WRF381P	reasonable	good	2.15 (1.9…2.12)	-0.1 (-0.28…-0.04)	reasonable

EC-EARTH_r1_COSMO-crCLIM-v1-1	good	good	1.22 (1.13…1.35)	-0.06 (-0.28…-0.11)	reasonable
EC-EARTH_r1_HIRHAM5	reasonable	good	1.16 (1.05…1.25)	-0.05 (-0.23…0.02)	bad
EC-EARTH_r1_RACMO22E	bad	reasonable	1.21 (1.07…1.4)	-0.01 (-0.19…0.05)	bad
EC-EARTH_r1_RCA4	reasonable	reasonable	1.31 (1.1…1.45)	-0.1 (-0.15…0.06)	reasonable
EC-EARTH_r12_CCLM4-8-17	good	good	1.44 (1.42…1.72)	-0.03 (-0.16…-0.02)	good
EC-EARTH_r12_COSMO-crCLIM-v1-1	good	good	1.39 (1.33…1.55)	-0.38 (-0.43…-0.35)	reasonable
EC-EARTH_r12_HadREM3-GA7-05	good	good	1.08 (0.97…1.03)	-0.02 (-0.04…0.03)	bad
EC-EARTH_r12_HIRHAM5	reasonable	good	0.95 (0.82…1.02)	-0.07 (-0.19…-0.05)	bad
EC-EARTH_r12_RACMO22E	bad	reasonable	1.13 (1.01…1.32)	-0.03 (-0.1…0.14)	bad
EC-EARTH_r12_RCA4	reasonable	reasonable	0.99 (0.77…1.08)	0.06 (-0.08…0.16)	bad
EC-EARTH_r12_RegCM4-6	good	good	1.16 (1.03…1.33)	0.01 (-0.05…0.12)	reasonable
EC-EARTH_r12_REMO2015	good	good	1.59 (1.42…1.59)	-0.19 (-0.28…-0.15)	good
EC-EARTH_r12_WRF361H	reasonable	reasonable	0.93 (0.87…1.05)	-0.34 (-0.79…-0.28)	bad
EC-EARTH_r12_WRF381P	good	good	1.49 (1.27…1.65)	0.06 (-0.14…0.18)	good
EC-EARTH_r3_COSMO-crCLIM-v1-1	good	good	1.49 (1.35…1.55)	-0.23 (-0.43…-0.2)	good
EC-EARTH_r3_HIRHAM5	reasonable	good	1.27 (1.22…1.46)	-0.3 (-0.38…-0.19)	reasonable
EC-EARTH_r3_RACMO22E	bad	reasonable	1.26 (1.21…1.29)	-0.15 (-0.24…-0.07)	bad
HadGEM2-ES_r1_ALADIN63	good	good	1.87 (1.53…1.97)	-0.08 (-0.15…0.11)	good
HadGEM2-ES_r1_CCLM4-8-17	reasonable	good	2.1 (1.85…2.07)	-0.25 (-0.26…-0.14)	reasonable
HadGEM2-ES_r1_COSMO-crCLIM-v1-1	reasonable	good	1.92 (1.51…2.16)	-0.13 (-0.2…0)	reasonable
HadGEM2-ES_r1_HadREM3-GA7-05	good	good	1.63 (1.54…1.87)	-0.04 (-0.33…-0.04)	good
HadGEM2-ES_r1_HIRHAM5	good	good	1.53 (1.53…1.74)	-0.09 (-0.21…-0.06)	good
HadGEM2-ES_r1_RACMO22E	good	good	1.7 (1.39…1.85)	0.06 (-0.05…0.21)	good
HadGEM2-ES_r1_RCA4	good	good	1.42 (1.28…1.7)	0.03 (-0.04…0.09)	good
HadGEM2-ES_r1_RegCM4-6	reasonable	good	1.22 (1.07…1.49)	0.24 (0.08…0.33)	reasonable
HadGEM2-ES_r1_REMO2015	reasonable	good	2 (1.66…2.11)	-0.26 (-0.4…-0.09)	reasonable
HadGEM2-ES_r1_WRF361H	good	good	1.48 (1.22…1.67)	0.04 (-0.1…0.08)	good

HadGEM2-ES_r1_WRF381P	good	good	1.82 (1.65…1.93)	0.11 (0.02…0.27)	good
IPSL-CM5A-MR_r1_HIRHAM5	bad	reasonable	1.48 (1.31…1.56)	-0.14 (-0.18…-0.07)	bad
IPSL-CM5A-MR_r1_RACMO22E	bad	reasonable	1.32 (1.06…1.41)	0.01 (0…0.22)	bad
IPSL-CM5A-MR_r1_RCA4	bad	reasonable	1.35 (1.39…1.75)	-0.27 (-0.44…-0.28)	bad
IPSL-CM5A-MR_r1_REMO2015	reasonable	reasonable	1.73 (1.48…1.97)	-0.03 (-0.18…0.03)	reasonable
IPSL-CM5A-MR_r1_WRF381P	reasonable	reasonable	2.69 (2.54…2.76)	-0.19 (-0.25…-0.18)	bad
MIROC5_r1_CCLM4-8-17	reasonable	good	1.7 (1.53…1.76)	-0.18 (-0.24…-0.05)	reasonable
MIROC5_r1_REMO2015	reasonable	good	1.69 (1.56…1.94)	-0.32 (-0.52…-0.26)	reasonable
MPI-ESM-LR_r1_ALADIN63	good	good	2.07 (1.78…2)	-0.09 (-0.15…0.08)	good
MPI-ESM-LR_r1_CCLM4-8-17	reasonable	reasonable	1.99 (1.86…2.21)	-0.1 (-0.11…0.01)	reasonable
MPI-ESM-LR_r1_COSMO-crCLIM-v1-1	good	good	1.83 (1.65…2.12)	-0.21 (-0.48…-0.12)	good
MPI-ESM-LR_r1_HadREM3-GA7-05	good	good	1.71 (1.59…1.89)	-0.08 (-0.14…0.1)	good
MPI-ESM-LR_r1_HIRHAM5	reasonable	reasonable	1.57 (1.4…1.64)	-0.12 (-0.29…-0.04)	reasonable
MPI-ESM-LR_r1_RACMO22E	bad	reasonable	1.61 (1.59…1.72)	-0.08 (-0.14…0)	bad
MPI-ESM-LR_r1_RCA4	bad	reasonable	1.31 (1.24…1.72)	-0.11 (-0.49…-0.01)	bad
MPI-ESM-LR_r1_RegCM4-6	good	good	1.38 (1.26…1.58)	0.1 (0.02…0.2)	good
MPI-ESM-LR_r1_REMO2009	good	reasonable	2.17 (1.85…2.36)	-0.21 (-0.23…-0.11)	reasonable
MPI-ESM-LR_r1_WRF361H	reasonable	good	1.39 (1.35…1.62)	0.06 (-0.07…0.13)	reasonable
MPI-ESM-LR_r2_COSMO-crCLIM-v1-1	reasonable	good	1.78 (1.58…1.93)	-0.28 (-0.3…-0.23)	reasonable
MPI-ESM-LR_r2_RCA4	bad	reasonable	1.13 (0.98…1.27)	0.05 (-0.05…0.15)	bad
MPI-ESM-LR_r2_REMO2009	good	good	1.73 (1.58…1.93)	-0.09 (-0.26…0)	good
MPI-ESM-LR_r3_COSMO-crCLIM-v1-1	good	good	1.49 (1.34…1.54)	-0.17 (-0.24…-0.02)	good
MPI-ESM-LR_r3_RCA4	bad	reasonable	1.06 (1.04…1.2)	-0.11 (-0.31…-0.06)	bad
MPI-ESM-LR_r3_REMO2015	good	good	1.73 (1.42…1.93)	-0.1 (-0.17…0.15)	good
NorESM1-M_r1_ALADIN63	reasonable	good	1.33 (1.12…1.37)	0.06 (0.11…0.23)	reasonable
NorESM1-M_r1_COSMO-crCLIM-v1-1	good	good	1.33 (1.12…1.43)	-0.21 (-0.3…-0.14)	good
NorESM1-M_r1_HadREM3-GA7-05	good	good	1.2 (1.1…1.28)	-0.07 (-0.13…-0.02)	reasonable
NorESM1-M_r1_HIRHAM5	reasonable	good	1.11 (1…1.14)	-0.12 (-0.19…-0.04)	bad

NorESM1-M_r1_RACMO22E	bad	reasonable	1.13 (0.96…1.2)	-0.05 (-0.14…0.02)	bad
NorESM1-M_r1_RCA4	bad	good	1.13 (1.02…1.19)	-0.1 (-0.29…-0.05)	bad
NorESM1-M_r1_RegCM4-6	good	good	1.27 (1.1…1.39)	-0.12 (-0.45…-0.1)	reasonable
NorESM1-M_r1_REMO2015	good	good	1.53 (1.41…1.63)	-0.13 (-0.15…0.04)	good
NorESM1-M_r1_WRF381P	reasonable	good	1.13 (0.93…1.19)	-0.05 (-0.03…0.06)	bad

Table A.1: Evaluation results of the climate models considered for attribution analysis of Tx2x over the study region. Results of a visual evaluation of the seasonal cycle and spatial pattern are given. For each model, the best estimate of the Sigma and Shape parameters are shown, and a 95% confidence interval is given for each, obtained via bootstrapping. The qualitative evaluation is shown in the right-hand column. Models used are highlighted in green, and the models not used are in yellow.

Model / Observations	Seasonal cycle	Spatial pattern	Sigma	Shape	Summary
cpc			1.72 (1.21…2.14)	0.06 (-0.3…0.38)	
EOBS			1.66 (1.39…1.92)	-0.02 (-0.21…0.14)	
era5			1.58 (1.29…1.87)	-0.08 (-0.28…0.1)	
MEgrid			1.65 (1.28…1.98)	-0.06 (-0.29…0.19)	
CNRM-CM5_r1_ALADIN63	reasonable	good	1.64 (1.44…1.79)	-0.05 (-0.09…-0.01)	reasonable
CNRM-CM5_r1_CCLM4-8-17	reasonable	good	1.87 (1.58…1.95)	-0.15 (-0.25…0.07)	reasonable
CNRM-CM5_r1_HadREM3-GA7-05	reasonable	good	1.6 (1.43…1.63)	-0.14 (-0.17…0.02)	reasonable
CNRM-CM5_r1_HIRHAM5	reasonable	good	1.39 (1.16…1.64)	-0.27 (-0.5…-0.08)	reasonable
CNRM-CM5_r1_RACMO22E	reasonable	reasonable	1.65 (1.4…1.69)	-0.18 (-0.22…0.03)	reasonable
CNRM-CM5_r1_RCA4	reasonable	good	1.45 (1.18…1.41)	-0.08 (-0.15…-0.02)	reasonable
CNRM-CM5_r1_REMO2015	reasonable	good	1.6 (1.28…1.92)	-0.19 (-0.44…0.01)	reasonable
CNRM-CM5_r1_WRF381P	reasonable	good	2.15 (1.9…2.12)	-0.1 (-0.28…-0.04)	reasonable
EC-EARTH_r1_COSMO-crCLIM-v1-1	good	good	1.22 (1.13…1.35)	-0.06 (-0.28…-0.11)	good
EC-EARTH_r1_HIRHAM5	reasonable	good	1.16 (1.05…1.25)	-0.05 (-0.23…0.02)	reasonable
EC-EARTH_r1_RACMO22E	bad	reasonable	1.21 (1.07…1.4)	-0.01 (-0.19…0.05)	bad
EC-EARTH_r1_RCA4	reasonable	reasonable	1.31 (1.1…1.45)	-0.1 (-0.15…0.06)	reasonable
EC-EARTH_r12_CCLM4-8-17	good	good	1.44 (1.42…1.72)	-0.03 (-0.16…-0.02)	good
EC-EARTH_r12_COSMO-crCLIM-v1-1	good	good	1.39 (1.33…1.55)	-0.38 (-0.43…-0.35)	bad

EC-EARTH_r12_HadREM3-GA7-05	good	good	1.08 (0.97…1.03)	-0.02 (-0.04…0.03)	bad
EC-EARTH_r12_HIRHAM5	reasonable	good	0.95 (0.82…1.02)	-0.07 (-0.19…-0.05)	bad
EC-EARTH_r12_RACMO22E	bad	reasonable	1.13 (1.01…1.32)	-0.03 (-0.1…0.14)	bad
EC-EARTH_r12_RCA4	reasonable	reasonable	0.99 (0.77…1.08)	0.06 (-0.08…0.16)	bad
EC-EARTH_r12_RegCM4-6	good	good	1.16 (1.03…1.33)	0.01 (-0.05…0.12)	reasonable
EC-EARTH_r12_REMO2015	good	good	1.59 (1.42…1.59)	-0.19 (-0.28…-0.15)	good
EC-EARTH_r12_WRF361H	reasonable	reasonable	0.93 (0.87…1.05)	-0.34 (-0.79…-0.28)	bad
EC-EARTH_r12_WRF381P	good	good	1.49 (1.27…1.65)	0.06 (-0.14…0.18)	good
EC-EARTH_r3_COSMO-crCLIM-v1-1	good	good	1.49 (1.35…1.55)	-0.23 (-0.43…-0.2)	good
EC-EARTH_r3_HIRHAM5	reasonable	good	1.27 (1.22…1.46)	-0.3 (-0.38…-0.19)	reasonable
EC-EARTH_r3_RACMO22E	bad	reasonable	1.26 (1.21…1.29)	-0.15 (-0.24…-0.07)	bad
HadGEM2-ES_r1_ALADIN63	good	good	1.87 (1.53…1.97)	-0.08 (-0.15…0.11)	good
HadGEM2-ES_r1_CCLM4-8-17	reasonable	good	2.1 (1.85…2.07)	-0.25 (-0.26…-0.14)	reasonable
HadGEM2-ES_r1_COSMO-crCLIM-v1-1	reasonable	good	1.92 (1.51…2.16)	-0.13 (-0.2…0)	reasonable
HadGEM2-ES_r1_HadREM3-GA7-05	good	good	1.63 (1.54…1.87)	-0.04 (-0.33…-0.04)	good
HadGEM2-ES_r1_HIRHAM5	good	good	1.53 (1.53…1.74)	-0.09 (-0.21…-0.06)	good
HadGEM2-ES_r1_RACMO22E	good	good	1.7 (1.39…1.85)	0.06 (-0.05…0.21)	good
HadGEM2-ES_r1_RCA4	good	good	1.42 (1.28…1.7)	0.03 (-0.04…0.09)	good
HadGEM2-ES_r1_RegCM4-6	reasonable	good	1.22 (1.07…1.49)	0.24 (0.08…0.33)	reasonable
HadGEM2-ES_r1_REMO2015	reasonable	good	2 (1.66…2.11)	-0.26 (-0.4…-0.09)	reasonable
HadGEM2-ES_r1_WRF361H	good	good	1.48 (1.22…1.67)	0.04 (-0.1…0.08)	good
HadGEM2-ES_r1_WRF381P	good	good	1.82 (1.65…1.93)	0.11 (0.02…0.27)	good
IPSL-CM5A-MR_r1_HIRHAM5	bad	reasonable	1.48 (1.31…1.56)	-0.14 (-0.18…-0.07)	bad
IPSL-CM5A-MR_r1_RACMO22E	bad	reasonable	1.32 (1.06…1.41)	0.01 (0…0.22)	bad
IPSL-CM5A-MR_r1_RCA4	bad	reasonable	1.35 (1.39…1.75)	-0.27 (-0.44…-0.28)	bad
IPSL-CM5A-MR_r1_REMO2015	reasonable	reasonable	1.73 (1.48…1.97)	-0.03 (-0.18…0.03)	reasonable
IPSL-CM5A-MR_r1_WRF381P	reasonable	reasonable	2.69 (2.54…2.76)	-0.19 (-0.25…-0.18)	bad
MIROC5_r1_CCLM4-8-17	reasonable	good	1.7 (1.53…1.76)	-0.18 (-0.24…-0.05)	reasonable

MIROC5_r1_REMO2015	reasonable	good	1.69 (1.56…1.94)	-0.32 (-0.52…-0.26)	bad
MPI-ESM-LR_r1_ALADIN63	good	good	2.07 (1.78…2)	-0.09 (-0.15…0.08)	good
MPI-ESM-LR_r1_CCLM4-8-17	reasonable	reasonable	1.99 (1.86…2.21)	-0.1 (-0.11…0.01)	reasonable
MPI-ESM-LR_r1_COSMO-crCLIM-v1-1	good	good	1.83 (1.65…2.12)	-0.21 (-0.48…-0.12)	good
MPI-ESM-LR_r1_HadREM3-GA7-05	good	good	1.71 (1.59…1.89)	-0.08 (-0.14…0.1)	good
MPI-ESM-LR_r1_HIRHAM5	reasonable	reasonable	1.57 (1.4…1.64)	-0.12 (-0.29…-0.04)	reasonable
MPI-ESM-LR_r1_RACMO22E	bad	reasonable	1.61 (1.59…1.72)	-0.08 (-0.14…0)	bad
MPI-ESM-LR_r1_RCA4	bad	reasonable	1.31 (1.24…1.72)	-0.11 (-0.49…-0.01)	bad
MPI-ESM-LR_r1_RegCM4-6	good	good	1.38 (1.26…1.58)	0.1 (0.02…0.2)	good
MPI-ESM-LR_r1_REMO2009	good	reasonable	2.17 (1.85…2.36)	-0.21 (-0.23…-0.11)	reasonable
MPI-ESM-LR_r1_WRF361H	reasonable	good	1.39 (1.35…1.62)	0.06 (-0.07…0.13)	reasonable
MPI-ESM-LR_r2_COSMO-crCLIM-v1-1	reasonable	good	1.78 (1.58…1.93)	-0.28 (-0.3…-0.23)	reasonable
MPI-ESM-LR_r2_RCA4	bad	reasonable	1.13 (0.98…1.27)	0.05 (-0.05…0.15)	bad
MPI-ESM-LR_r2_REMO2009	good	good	1.73 (1.58…1.93)	-0.09 (-0.26…0)	good
MPI-ESM-LR_r3_COSMO-crCLIM-v1-1	good	good	1.49 (1.34…1.54)	-0.17 (-0.24…-0.02)	good
MPI-ESM-LR_r3_RCA4	bad	reasonable	1.06 (1.04…1.2)	-0.11 (-0.31…-0.06)	bad
MPI-ESM-LR_r3_REMO2015	good	good	1.73 (1.42…1.93)	-0.1 (-0.17…0.15)	good
NorESM1-M_r1_ALADIN63	reasonable	good	1.33 (1.12…1.37)	0.06 (0.11…0.23)	reasonable
NorESM1-M_r1_COSMO-crCLIM-v1-1	good	good	1.33 (1.12…1.43)	-0.21 (-0.3…-0.14)	good
NorESM1-M_r1_HadREM3-GA7-05	good	good	1.2 (1.1…1.28)	-0.07 (-0.13…-0.02)	reasonable
NorESM1-M_r1_HIRHAM5	reasonable	good	1.11 (1…1.14)	-0.12 (-0.19…-0.04)	bad
NorESM1-M_r1_RACMO22E	bad	reasonable	1.13 (0.96…1.2)	-0.05 (-0.14…0.02)	bad
NorESM1-M_r1_RCA4	bad	good	1.13 (1.02…1.19)	-0.1 (-0.29…-0.05)	bad
NorESM1-M_r1_RegCM4-6	good	good	1.27 (1.1…1.39)	-0.12 (-0.45…-0.1)	good
NorESM1-M_r1_REMO2015	good	good	1.53 (1.41…1.63)	-0.13 (-0.15…0.04)	good
NorESM1-M_r1_WRF381P	reasonable	good	1.13 (0.93…1.19)	-0.05 (-0.03…0.06)	bad

Table A.2: Evaluation results of the climate models considered for attribution analysis of Tx1x over the study region. Results of a visual evaluation of the seasonal cycle and spatial pattern are given. For each model, the best estimate of the Sigma and Shape parameters are shown, and a 95% confidence

interval is given for each, obtained via bootstrapping. The qualitative evaluation is shown in the right-hand column. Models used are highlighted in green, and the models not used are in yellow.

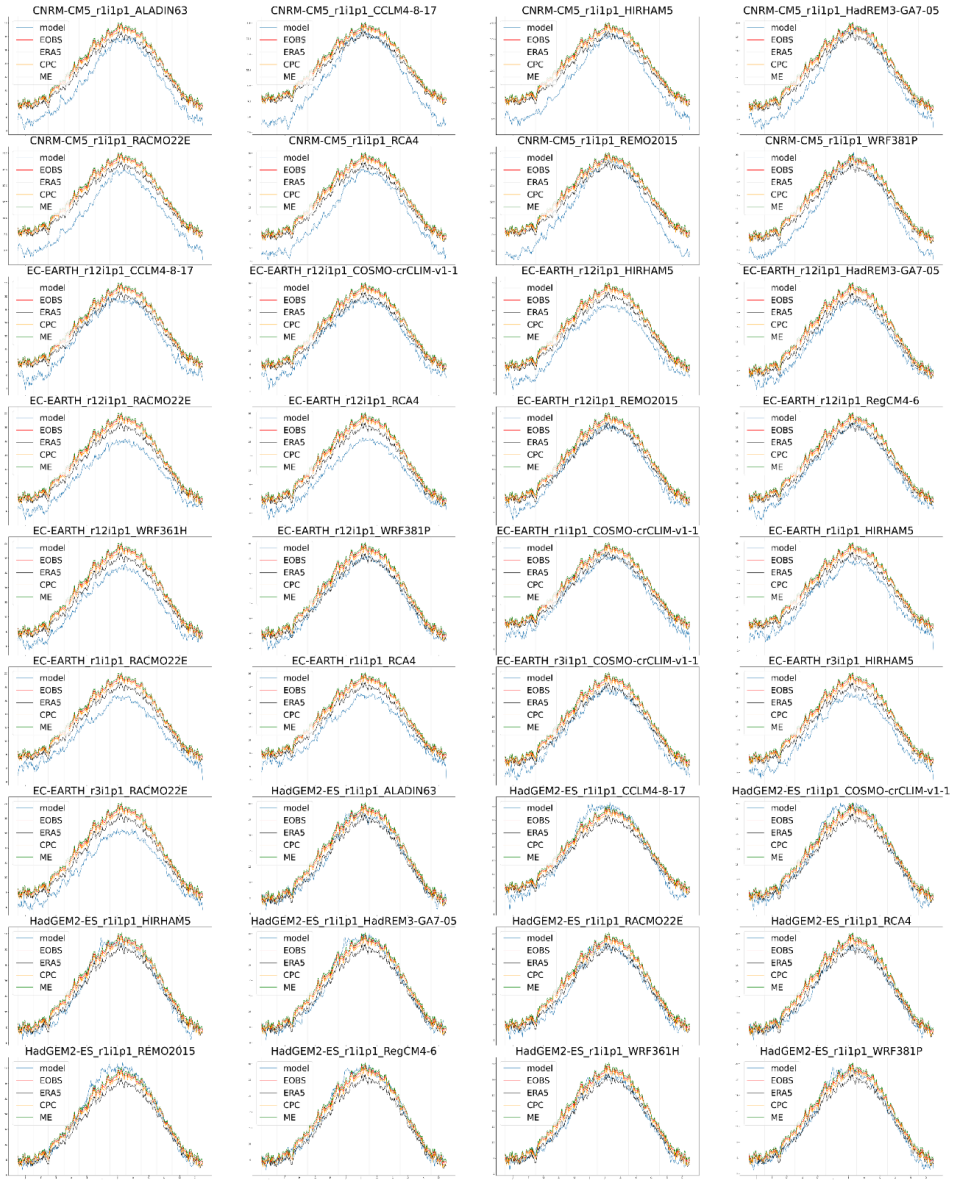

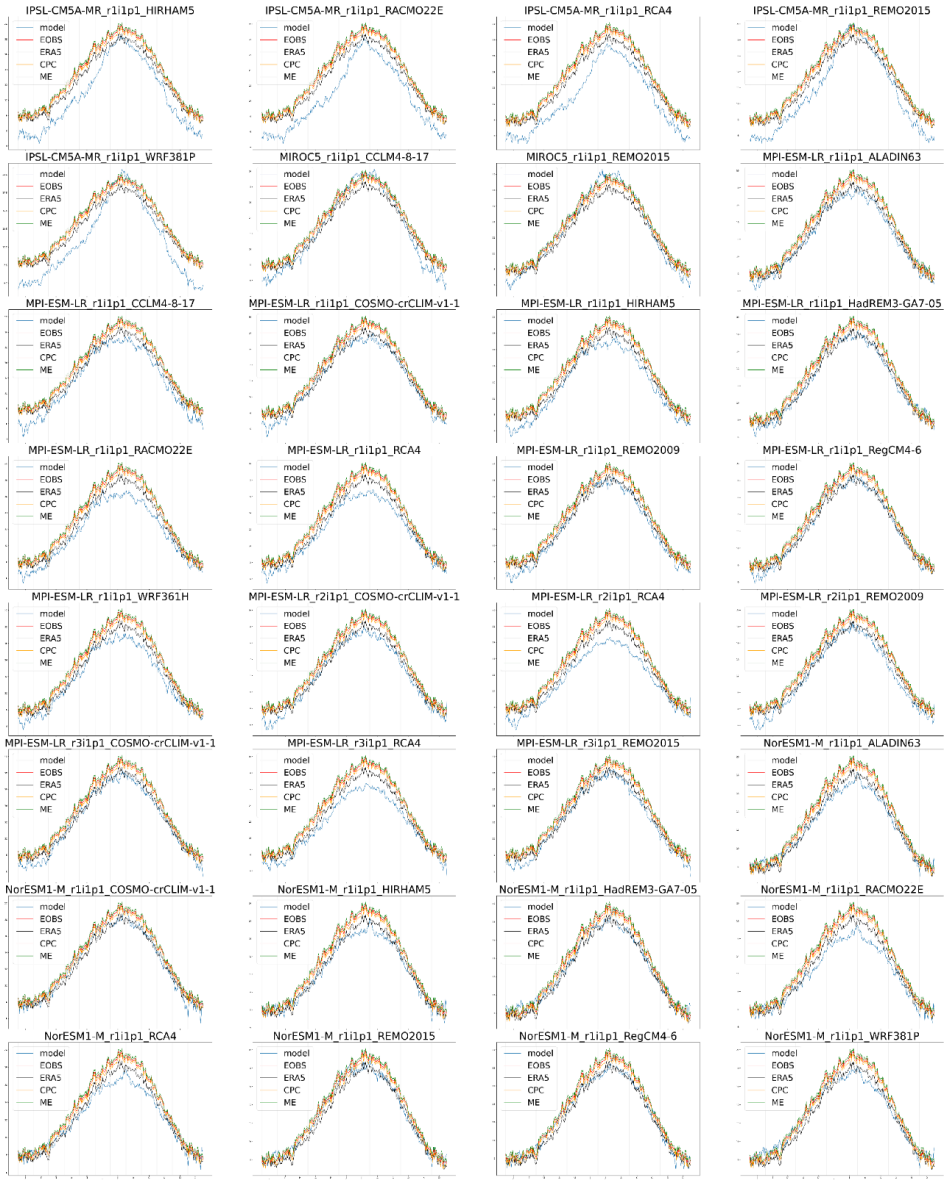

Figure A.3: Seasonal cycles of daily maximum temperatures in observations, EOBS shown in red, ERA5 shown in black, CPC in yellow, Met Éireann in green, and CORDEX models, shown in blue.

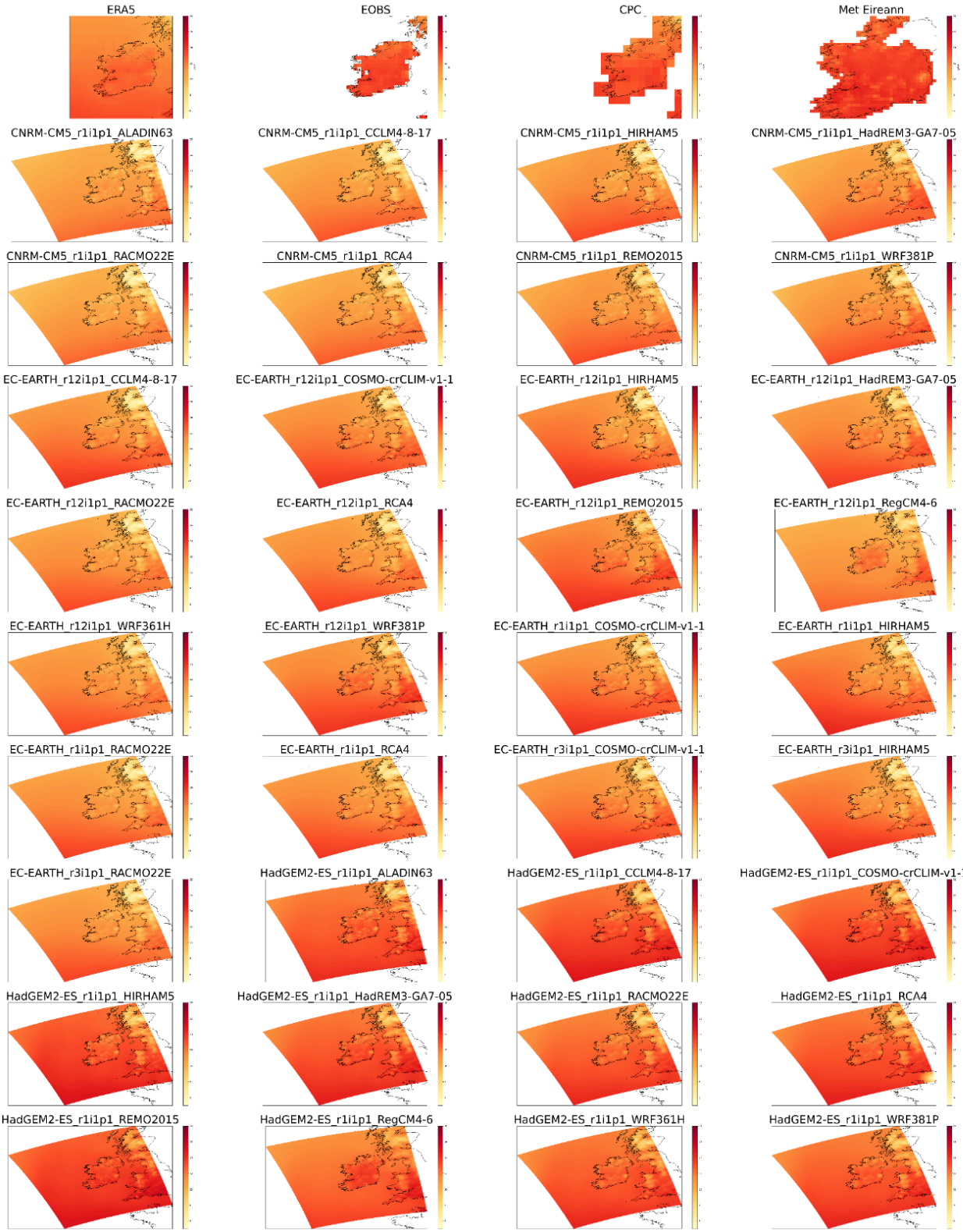
ERA5
EOBS
CPC
Met Eireann
CNRM-CM5_r1i1p1_ALADIN63
CNRM-CM5_r1i1p1_CCLM4-8-17
CNRM-CM5_r1i1p1_HIRHAM5
CNRM-CM5_r1i1p1_HadREM3-GA7-05
CNRM-CM5_r1i1p1_RACMO22E
CNRM-CM5_r1i1p1_RCA4
CNRM-CM5_r1i1p1_REMO2015
CNRM-CM5_r1i1p1_WRF381P
EC-EARTH_r12i1p1_CCLM4-8-17
EC-EARTH_r12i1p1_COSMO-crCLIM-v1-1
EC-EARTH_r12i1p1_HIRHAM5
EC-EARTH_r12i1p1_HadREM3-GA7-05
EC-EARTH_r12i1p1_RACMO22E
EC-EARTH_r12i1p1_RCA4
EC-EARTH_r12i1p1_REMO2015
EC-EARTH_r12i1p1_RegCM4-6
EC-EARTH_r12i1p1_WRF361H
EC-EARTH_r12i1p1_WRF381P
EC-EARTH_r1i1p1_COSMO-crCLIM-v1-1
EC-EARTH_r1i1p1_HIRHAM5
EC-EARTH_r1i1p1_RACMO22E
EC-EARTH_r1i1p1_RCA4
EC-EARTH_r3i1p1_COSMO-crCLIM-v1-1
EC-EARTH_r3i1p1_HIRHAM5
EC-EARTH_r3i1p1_RACMO22E
HadGEM2-ES_r1i1p1_ALADIN63
HadGEM2-ES_r1i1p1_CCLM4-8-17
HadGEM2-ES_r1i1p1_COSMO-crCLIM-v1-1
HadGEM2-ES_r1i1p1_HIRHAM5
HadGEM2-ES_r1i1p1_HadREM3-GA7-05
HadGEM2-ES_r1i1p1_RACMO22E
HadGEM2-ES_r1i1p1_RCA4
HadGEM2-ES_r1i1p1_REMO2015
HadGEM2-ES_r1i1p1_RegCM4-6
HadGEM2-ES_r1i1p1_WRF361H
HadGEM2-ES_r1i1p1_WRF381P

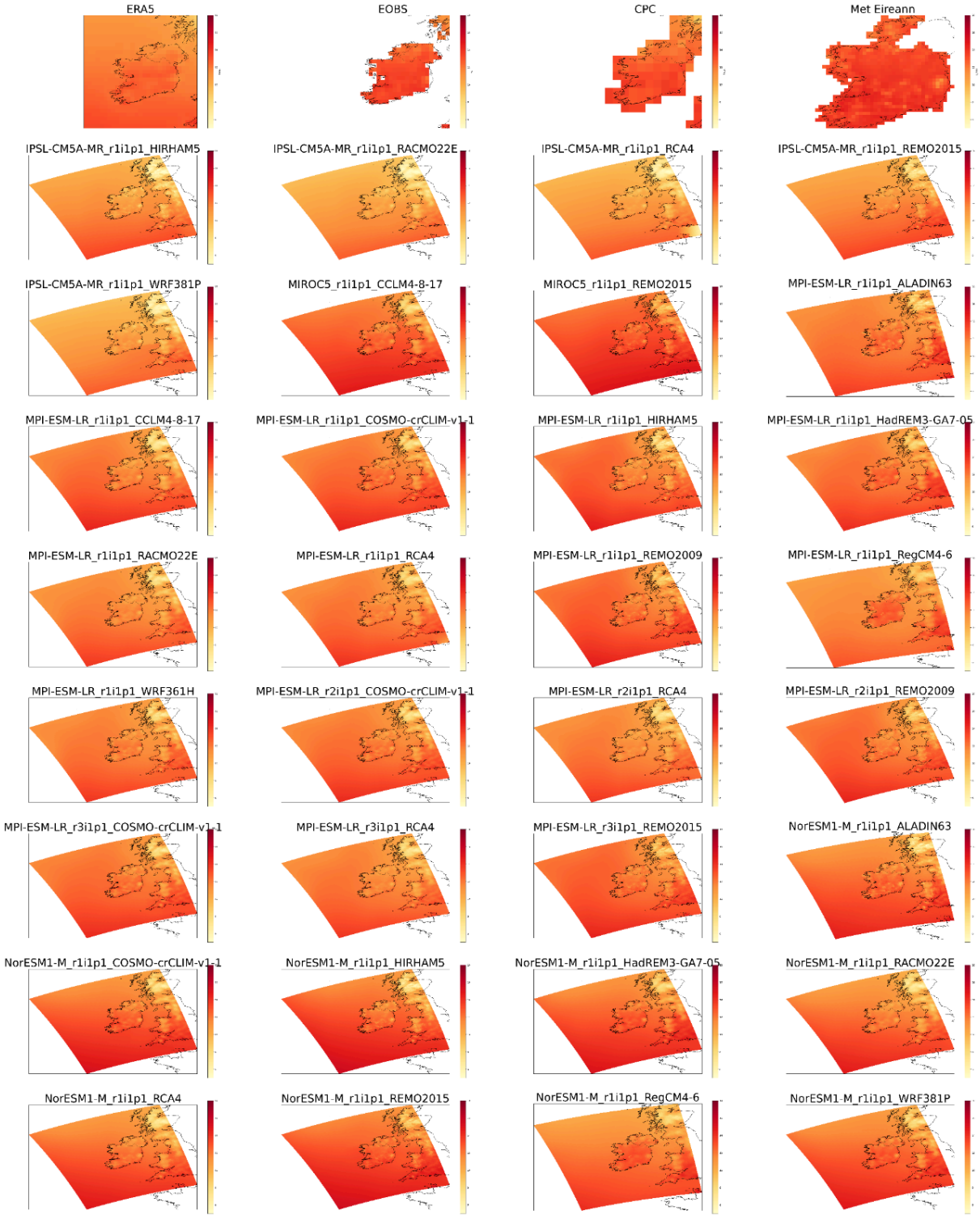

Figure A.4: Spatial patterns of daily maximum temperatures in observations and CORDEX models.